MINISTERIO DE INDUSTRIA Y ENERGIA
SECRETARIA DE LA ENERGIA Y RECURSOS MINERALES

ANALISIS METODOLOGICO DE LAS TECNICAS GEOQUIMICAS EMPLEADAS EN PROSPECCION GEOTERMICA

" A P E N D I C E A "

"Application of Water Geochemistry to Geothermal and Reservoir Engineering". By R.O. Fournier

INSTITUTO GEOLOGICO Y MINERO DE ESPAÑA

Julio 1985

ANALISIS METODOLOGICO DE LAS TECNICAS GEOQUIMICAS EMPLEADAS EN PROSPECCION GEOTERMICA

" A P E N D I C E A "

"Application of Water Geochemistry to Geothermal and Reservoir Engineering". By R.O. Fournier

Appendix 5A

Application of Water Geochemistry to Geothermal Exploration and Reservoir Engineering*

by
Robert O. Fournier
U. S. Geological Survey

INTRODUCTION

The application of geochemistry to the development of geothermal energy is a big subject encompassing many facets. In this chapter emphasis will be placed upon the use of water chemistry to determine underground temperatures and boiling and mixing relations in the exploration and production phases of geothermal energy utilization. Although knowledge of the composition and behavior of gas associated with hot water is of very great interest and practical importance, gas geochemistry will not be discussed here.

Thermal energy serves as an engine that sets water in the earth's crust into convective motion, forming what we call hydrothermal systems. Water may become heated owing to deep circulation along favorable structures in regions of normal geothermal gradient or by interaction with magmas and cooling igneous rocks that have intruded to relatively shallow levels in the crust.

The explored parts of most presently active hydrothermal systems are dominated by meteoric or ocean water that has changed composition during underground movement in response to changing temperature, pressure, and rock type. Changing temperature has a major effect upon the ratios of cations in solution and the concentration of dissolved silica. Changing pressure is an important factor in regard to evaporative concentration and partitioning of volatile components between water and steam during boiling. Variations in rock type strongly influence the total salinity and particularly the chloride concentration that a hydrothermal solution is likely to attain.

*In: Geothermal Systems: Principles and Case Histories
Edited by L. Rybach and L. P. Muffler
1980 John Wiley a Sons Ltd., p. 109-143

HYDROTHERMAL REACTIONS

The compositions of geothermal fluids are controlled by temperature dependent reactions between minerals and fluids. In order to understand and model hydrothermal systems both the fluid and solids must be characterized.

Browne (1978) summarized the factors affecting the formation of hydrothermal minerals as follows: (a) temperature, (b) pressure, (c) rock type, (d) permeability, (e) fluid composition, and (f) duration of activity. He further stated that the effects of rock type were most pronounced at low temperatures and generally insignificant above 280°C. Above 280°C and at least as high as 350°C the typical stable mineral assemblage found in active geothermal systems is not dependent on original rock type and includes albite, K-feldspar, chlorite, Fe-epidote, calcite, quartz, illite, and pyrite. At lower temperatures many different zeolites and clay minerals also are found. Apparently epidote does not form below about 240°C, although in some places it may persist metastably at lower temperatures. Where permeability is low equilibrium between rocks and reservoir fluids is seldom achieved and unstable primary minerals or glass can persist at high temperatures. Metastable minerals also form and persist in some geothermal systems, particularly where glassy rocks are present and temperatures are below about 200°C.

In geothermal reservoirs where permeabilities are relatively high and water residence times are long (months to years), water and rock should reach chemical equilibrium, especially where temperatures exceed 200°C. At equilibrium, ratios of cations in solution are controlled by temperature-dependent exchange reactions such as

Albite K-feldspar

$$NaAlSi_3O_8 + K^+ = KAlSi_3O_8 + Na^+, \quad (1)$$

$$K_{eq} = \frac{[Na^+]}{[K^+]}, \quad (2)$$

and

Wairakite Quartz Albite

$$CaAl_2Si_4O_{12} \cdot 2H_2O + 2SiO_2 + 2Na^+ = 2NaAlSi_3O_8 + Ca^{++} + 2H_2O, \quad (3)$$

$$K_{eq} = \frac{[Ca^{++}][H_2O]^2}{[Na^+]^2}. \quad (4)$$

Hydrogen ion activity (pH) is controlled by hydrolysis reactions, such as

K-feldspar K-mica Quartz

$$3KAlSi_3O_8 + 2H^+ = KAl_3Si_3O_{10}(OH)_2 + 6SiO_2 + 2K^+, \quad (5)$$

$$K_{eq} = \frac{[K^+]}{[H^+]}, \quad (6)$$

Albite Na-Montmorillonite Quartz

$$2.33NaAlSi_3O_8 + 2H^+ = Na_{.33}Al_{2.33}Si_{3.67}O_{10}(OH)_2 + 3.33SiO_2 + 2Na^+, \quad (7)$$

$$K_{eq} = \frac{[Na^+]}{[H^+]}, \quad (8)$$

and

Wairakite Ca-Montmorillonite

$$1.17CaAl_2Si_4O_{12}\cdot 2H_2O + 2H^+ = Ca_{.17}Al_{2.33}Si_{3.67}O_{10}(OH)_2 +$$

Quartz

$$SiO_2 + 2H_2O + Ca^{++} \quad (9)$$

$$K_{eq} = \frac{[Ca^{++}]\,[H_2O]^2}{[H^+]^2}. \quad (10)$$

In the above equations K_{eq} is the equilibrium constant for the given reaction, asssuming unit activities of the solid phases, and square brackets indicate activities of the dissolved species. The extent to which natural water-rock systems approach chemical equilibrium can be tested by comparing actual compositions of fluids and minerals found in drilled geothermal reservoirs with theoretical compositions calculated using thermodynamic data (Helgeson, 1969; Helgeson et al., 1969; Robie et al., 1978).

The first step in testing water-rock equilibration is to collect and analyze of representative fluid and rock samples (Ellis and Mahon, 1977; Watson, 1978) from a reservoir at a known temperature. Cuttings and core are collected during drilling, although sidewall cores can be collected later. Core is preferred over cuttings for mineralogic work because paragenetic relations are clearer, and minerals that occur only in veins can be distinguished from those only in the rock matrix. Also, with cuttings, one cannot be sure that all the fragments come from the same interval of rock. Fragments from higher in the hole may become incorporated in the drilling mud along with cuttings from the bottom of the well.

Fluid samples are collected after drilling mud and makeup water have been flushed from the well. The best way to collect a water sample is with a downhole sampler, but wellhead samples can be used provided the water in the well comes from only one permeable zone. From the results of the chemical analyses combined with data on the conditions of sample collection, the original thermodynamic state of the fluid in the reservoir can be calculated using computer programs (Truesdell and Singers, 1974; Arnórsson, 1978) that correct for the presence of complex ions and the separation of steam. The natural and theoretical systems can be compared by noting the degree of saturation of the fluid in respect to each of the various minerals found in core and cuttings from the reservoir rocks, using a computer program (Kharaka and Barnes, 1973). A major limitation of this approach is that thermochemical data are not available for many of the zeolites, clays, and micas commonly

found in geothermal systems. Also, many of the minerals are solid solutions which presently available computer programs treat by assuming pure end-member compositions. Results of this type of procedure usually show that the solutions are saturated with respect to the observed minerals (those for which thermochemical data are available) within the limits of error of the method.

Another method of comparison is to determine where the activity ratios of aqueous species (calculated by computer) plot on theoretical activity diagrams (Helgeson et al., 1969) that depict mineral stability fields in chemically restricted systems. Ellis (1969), Browne and Ellis (1970) and Ellis and Mahon (1977) plot water compositions from Wairakei and Broadlands, N. Z. on a variety of activity diagrams. The diagram for Broadlands in terms of $[Na^+]/[H^+]$ and $[K^+]/[H^+]$ activity ratios at 260°C is shown in figure 1, and for $[K^+]/[H^+]$ and $[Ca^{++}]/[H^+]^2$ in figure 2. The Broadlands water composition shown in figure 1 plots close to the triple point of K-feldspar, K-mica, and albite, suggesting an approach to water-rock equilibrium involving those minerals at 260°C. In figure 2, the Broadlands water plots close to a triple point of K-feldspar, K-mica, and wairakite. Calcite also is present with 0.15 $\underline{m}$ CO_2 in the system. The maximum temperatures in wells at Broadlands usually are in the range 270° to 290°C. If figures 1 and 2 had been drawn for 290°C, the water composition would have plotted even closer to the triple points. Reasons, other than temperature, for slight discrepancies between actual solution compositions and theoretical equilibrium compositions involve uncertainties in the structural states of the reacting solids and limitations in our knowledge of all the possible complex ions that may be present at high temperatures in natural waters. The influence of structural state is illustrated in figure 3 which shows expected $[Na^+]/[K^+]$ activity ratios in solutions equilibrated with different alkali feldspar pairs at various temperatures. At 100°C, the value of $\log([Na^+]/[K^+])$ for the assemblage low-albite plus microcline is about 0.2 units lower than for the assemblage low-albite plus adularia and about 0.7 units lower than for the assemblage high-albite plus sanidine. Differences are still significant at 300°C; about 0.3 units.

The activity diagram method of presentation allows one to focus upon a few of the more important components in the system and to visualize the effects of changing one or more parameters. In figure 1, lowering the temperature while maintaining water-rock equilibrium would cause the solution to follow the path shown by the arrow. In figure 2 the effect of increasing CO_2 concentration is shown by the expanding field of calcite that completely replaces zoisite when $\underline{m}$ CO_2 = 0.03 and completely replaces wairakite when $\underline{m}$ CO_2 = 1.0.

ESTIMATION OF RESERVOIR TEMPERATURE

Many different chemical and isotopic reactions might be used as geochemical thermometers or geothermometers (Ellis and Mahon, 1977; Fournier 1977; Truesdell and Hulston, 1980) to estimate reservoir temperatures. At present the most widely used are silica (Fournier and Rowe, 1966; Mahon, 1966), Na/K (White, 1965; Ellis and Mahon, 1967; White, 1970; Truesdell, 1976a; Fournier, 1979a), Na-K-Ca (Fournier and Truesdell 1973), and sulfate oxygen isotope, $\Delta^{18}O(SO_4^{=} - H_2O)$, which uses the fractionation of oxygen isotopes between water and dissolved sulfate (Lloyd, 1968; Mizutani and Rafter, 1969; Mizutani, 1972; McKenzie and Truesdell, 1977). Equations expressing the temperature dependence of the above geothermometers are listed in table 1. It is relatively easy to compute temperatures using the equations in table 1. Interpreting the results of these computations, however, requires consideration of the geologic and hydrologic setting and the physical nature as well as complete chemical analysis of the fluid that was sampled. Some people find it dismaying that different geothermometers give different estimated temperatures. However, shrewd investigators will use that kind of information to their advantage when formulating a model of the hydrothermal system because different geothermometers may indicate temperatures in different parts of the system.

The Silica Geothermometer

Bodvarsson (1960) suggested an empirical, qualitative geothermometer based on the silica concentrations in natural thermal waters in Iceland. The experimental work of Morey et al. (1962) on the solubility of quartz in water at the vapor pressure of the solution, combined with higher temperature results of Kennedy (1950), provided a theoretical basis for the geothermometer (curve A in figure 4). Mahon (1966) showed that the silica concentrations in waters from geothermal wells in New Zealand are controlled by the solubility of quartz, and Fournier and Rowe (1966) described a method of using the silica concentration in hot-spring and well waters to make quantitative estimates of reservoir temperatures.

The quartz geothermometer works best for well waters where subsurface temperatures are above about 150°. It has been shown to work well for some hot spring waters (Fournier and Truesdell, 1970), but can give erroneous results when applied indiscriminately. The following factors should be considered when using the quartz geothermometer: (a) the temperature range in which the equations in table 1 are valid, (b) effects of steam separation, (c) possible polymerization and/or precipitation of silica before sample collection, (d) possible polymerization of silica after sample collection owing to improper preservation of the sample, (e) control of aqueous silica by solids other than quartz, (f) the effect of pH upon quartz solubility, and (g) possible dilution of hot water with cold water before the thermal water reaches the surface.

Temperature range of equations - The equations commonly used to describe the solubility of quartz at the vapor pressure of the solution (Morey et al., 1962; Fournier and Rowe, 1966; Truesdell, 1976a; Fournier, 1977) are good to about ±2°C over the temperature range 0°C to 250°C. Above 250°C the equations depart drastically from the experimentally determined solubility curve (Curve A in figure 4) and should not be used.

Effects of steam separation - As water boils, the silica concentration in the residual liquid increases in proportion to the amount of steam that separates. Thus, when applying the quartz geothermometer to boiling hot springs it is necessary to correct for the amount of steam formation or the proportion of adiabatic vs. conductive cooling, as outlined by Fournier and Rowe (1966). Vigorously boiling springs with mass flow rates grater than 120 to 130 kg/*min can* be assumed to have cooled mainly adiabatically (Truesdell et al., 1977), and equation b in table 1 (for maximum steam loss at 100 kPa pressure) or curve B in figure 4 can be used to estimate the reservoir temperature. If cooling was partly adiabatic and partly by conduction, the reservoir temperature should be between the temperatures given by equations a and b in table 1 or between the temperatures indicated by curves A and B in figure 4. For springs issuing high above sea level, final steam formation can occur at significantly less than 100 kPa, so that equation b in table 1 for maximum steam formation and curve B in figure 4 will give a calculated reservoir temperature that is slightly high.

Precipitation of silica prior to sample collection - The quartz geothermometer works because the rate of quartz precipitation decrease drastically as temperature decreases. In the temperature range 200°C to 250°C water reaches equilibrium with quartz in a few hours to a few days, depending on the solution temperature, pH, salinity, and degree of initial silica supersaturation or undersaturation. High salinity and pH in the range 5 to 8 favor faster reaction rates. Below 100°C, solutions may remain supersaturated with respect to quartz for years. When waters flow up to the surface from reservoirs with temperatures less than about 225°C to 250°C and cool fairly quickly (in less than a few hours), little quartz is likely to precipitate during the upflow. However, where reservoir temperatures are above 250°C, some quartz is likely to precipitate in the deep, hot part of the system as the solution cools. In addition, an ascending solution starting at temperatures above about 225°C will become supersaturated with respect to amorphous silica before reaching the surface owing to the decreased temperature, especially if adiabatic cooling takes place (figure 4). Amorphous silica precipitates much more quickly than quartz at comparable temperatures. Because of the precipitation of quartz at high temperatures and polymerization and precipitation of amorphous silica at low temperatures, the quartz geothermometer applied to hot spring waters seldom indicates temperatures exceeding 225-250°C, even where higher temperature reservoirs are known to exist.

Precipitation of silica after sample collection - The solubility of amorphous silica at 25°C is about 115 mg/kg (Morey et al., 1964). The solubility of quartz is 115 mg/kg at about 145°C (figure 4). Therefore, waters coming from reservoirs above 145°C will become supersaturated with respect to amorphous silica upon cooling to 25°C. At high temperatures all of the dissolved silica in equilibrium with quartz is in the monomeric form. When a cooling solution becomes saturated with respect to amorphous silica some of the monomeric silica usually converts to highly polymerized dissolved silica species, with or without the simultaneous precipitation of amorphous silica. Colorimetric methods of analysis used to determine dissolved silica are sensitive to monomeric silica, but fail to detect most highly polymerized forms of dissolved silica. To prevent silica polymerization and precipitation of amorphous silica, a known amount of the sample (5 to 10 ml) should be pipetted into about 50 ml of silica-free water immediately after sample collection.

Control of aqueous silica by solids other than quartz - Quartz is the most stable and least soluble polymorphic form of silica within the temperature and pressure range found in geothermal systems. However, for kinetic reasons other silica phases may form or persist metastably within the stability field of quartz. The solubilities of various silica phases in liquid water at the vapor pressure of the solution are shown in figure 5. Plots of log concentration vs. reciprocal of absolute temperature yield essentially straight lines below 250°C that make extrapolation of the data to lower temperatures very simple. Equations relating the solubility, C, in mg SiO_2 per kg water, to temperature for the various silica phases are given in table 1.

In most natural waters at temperatures above 150°C, and in some waters below that temperature, quartz appears to control the dissolved silica concentration. However, under special conditions for short periods of time any of the other silica species may control aqueous silica, even at very high temperatures. This conclusion is based upon (1) compositions of natural waters in drill holes; (2) paragenetic sequences of silica minerals in drill core from hot spring areas; and (3) laboratory investigations in which it has been found that as long as two different silica species contact the solution, e.g., quartz and glass, the more soluble one controls aqueous silica (Fournier, 1973).

In the basaltic terrain of Iceland, chalcedony generally controls aqueous silica at temperatures below 110°C and sometimes at temperatures as high as 180°C (Arnorsson, 1975). In some granite terrains aqueous silica is controlled by quartz at temperatures above 90°C and by chalcedony at lower temperatures (Christian Fouillac, oral commun., 1977).

Most groundwaters which have not attained temperatures greater than 80°C to 90°C have silica concentrations greater than those predicted by the solubility of quartz. Some of these low-temperature waters have equilibrated with chalcedony, as indicated above. However, the silica concentrations in many groundwaters result from non-equilibrium reactions in which silica is released to solution during acid alteration of silicate minerals (for example

equations 5, 7, and 9). At low temperatures, the rates of quartz and chalcedony precipitation are very slow so aqueous silica values may become high where acid is continually supplied from an outside source, such as by decay of organic material, oxidation of sulfides, or influx of H_2S or CO_2. According to Ivan Barnes and R. H. Mariner (written commun., 1975) cold waters with high silica concentrations (attaining saturation with respect to amorphous silica) and near neutral pH are particularly prevalent where CO_2 and water react with serpentine. This conclusion is in agreement with results of experimental studies by Wildman et al. (1968) in which serpentine was dissolved at 25°C at various pressures of CO_2.

Effect of pH - The effect of pH upon the solubility of quartz at various temperatures can be calculated from the work of Seward (1974) or Busey and Mesmer (1977), and is shown in figure 6. The dashed line in figure 6 shows pH values at which the solubility of quartz becomes ten percent greater than the solubility in water with pH = 7.0. A ten percent increase in dissolved silica owing to increased pH will cause silica geothermometer temperatures to be about 6° too high at 180° and about 12° too high at 250°C. At 25°C a pH of 8.9 is required to achieve a ten percent increase while at 100°C a pH of just 8.2 is required. The effect of pH upon quartz solubility is most pronounced at about 175°C where a pH of 7.6 will cause an increase in quartz solubility of ten percent. However, pH values of solutions in high-temperature geothermal reservoirs are likely to be below 7.5 because of buffering of hydrogen ions by silicate hydrolysis reactions such as shown by equations 5, 7, and 9. pH values higher than 7.5 in natural hot-spring waters generally result from the loss of CO_2 after the water leaves the high-temperature reservoir.

Whether or not a correction should be applied to adjust the silica concentration of an alkaline hot spring water for pH effects before applying the silica geothermometer depends upon where and when the solution attained its aqueous silica. If a solution became alkaline and then dissolved additional silica in response to the rise in pH, a pH correction is necessary. In contrast, if a solution attained a high silica concentration owing to high underground temperature and then became alkaline after cooling and loss of CO_2, no pH correction should be applied. In general, if there is other supporting evidence that a thermal water comes from a higher-temperature environment at depth, a pH correction should NOT be applied to the observed silica concentration.

Subsurface dilution of thermal water by cold water - In many places there is evidence that ascending thermal water becomes diluted by cooler water. A new water-rock chemical equilibrium may or may not be attained after mixing. If chemical equilibrium is attained after mixing, the silica geothermometer will give the temperature of that last equilibrium. If chemical equilibrium is not attained after mixing, direct application of the silica geothermometer will give a calculated temperature that is too low. Methods of dealing with diluted thermal waters will be discussed in the section on underground mixing and boiling.

The Na/K Geothermometer

Many investigators have noted the variation of Na^+ and K^+ in natural geothermal waters as a function of temperature (White, 1965, 1970; Ellis and Mahon, 1967; Ellis, 1970; Fournier and Truesdell, 1970, 1973; and Mercado, 1970). Figure 7 shows Na^+/K^+ mg/kg concentration ratios in waters from geothermal wells throughout the world, plotted at the respective measured reservoir temperatures. In figure 7, curves C and D show the approximate location (assuming activity ratios = 1.7 x mg/kg concentration ratios) of the low-albite plus microcline and high-albite plus sanidine curves from figure 3. Note that above 100°C most of the well waters plot between curves C and D. Below 100°C most well waters plot below curve C, indicating that the ratio of dissolved Na^+ to K^+ generally is not controlled by cation exchange between coexisting alkali feldspar pairs at low temperatures.

Line A, figure 7, is the least-squares best fit of the well water data points above 80°C. The data points at temperatures below 80°C were not included in the least squares fit because the Na/K method generally gives unreliable results at low temperatures.

The equation of curve A, figure 7, is labeled g in table 1. Truesdell (1976a) recommended using a combined curve of White (1965) and Ellis (1970) for geothermometry as drawn by Fournier and Truesdell (1973). That curve is shown as line B in figure 7 and its equation is labeled h in table 1.

At temperatures near 270°C it makes little difference whether curve A or curve B in figure 7 (equation g or h) is used for estimating temperatures. At temperatures between 125°C and 200°C, curve B departs significantly from most of the data points. Therefore, curve A is recommended for geothermometry instead of curve B. Curve B does come closer to most data points below 100°C, but it appears that the Na/K method generally fails to give reliable results for waters from environments with temperatures below 100°C. In particular, low-temperature waters rich in calcium give anomalous results by the Na/K method.

Where waters are known to come from high-temperature environments (>180°C to 200°C), the Na/K method generally gives excellent results. The main advantage of the Na/K geothermometer is that it is less affected by dilution and steam separation than other commonly used geothermometers, provided there is little Na^+ and K^+ in the diluting water compared to the reservoir water.

The Na-K-Ca Geothermometer

The Na-K-Ca geothermometer of Fournier and Truesdell (1973) was developed specifically to deal with calcium-rich waters that give anomalously high calculated temperatures by the Na/K method. An empirical equation giving the variation of temperature with Na, K, and Ca is listed in table 1, letter i.

When using equation i in Table 1, first calculate the temperature using a value of $\beta = 4/3$ and cation concentrations expressed either as mg/kg or ppm. If that calculated temperature is <100°C and $[\log(\sqrt{Ca}/Na) + 2.06]$ is positive, proceed no further. However, if the $\beta = 4/3$ calculated temperature is >100°C or if $[\log(\sqrt{Ca}/Na) + 2.06]$ is negative, use $\beta = 1/3$ to calculate the temperature.

Changes in concentration resulting both from boiling and from mixing with cold, dilute water will affect the Na-K-Ca geothermometer. The main consequence of boiling is loss of CO_2 which can cause $CaCO_3$ to precipitate. The loss of aqueous Ca^{++} generally will result in Na-K-Ca calculated temperatures that are too high.

The effect of dilution on the Na-K-Ca geothermometer is generally negligible if the high-temperature geothermal water is much more saline than the diluting water. However, if a particular water is thought to be a mixture of hot and cold water with less than 20 to 30 percent hot water component, the effects of mixing on the Na-K-Ca geothermometer should be considered. Figure 8 shows $\beta = 1/3$ and $\beta = 4/3$ Na-K-Ca geothermometer temperatures for various mixtures of two hypothetical waters, one starting at 210°C and the other at 10°C. A 50:50 mixture of the two waters would have an actual temperature of about 110°C and would give a $\beta = 4/3$ temperature of 143°C and a $\beta = 1/3$ temperature of 198°C. By the criteria of Fournier and Truesdell (1973) the $\beta = 1/3$ temperature would be selected as most likely. Thus, the Na-K-Ca geothermometer would give a temperature only 12°C below the actual 210°C temperature. However, when the amount of cold water in the mixture becomes greater than 75 percent, the $\beta = 4/3$ geothermometer temperature drops to less than 100°C and a hot spring would emerge at less than 60°C. Because the $\beta = 4/3$ temperature is less than 100°C, it normally would be selected as the more likely temperature of water-rock equilibration instead of the $\beta = 1/3$ temperature.

Fournier and Potter (1979) showed that the Na-K-Ca geothermometer gives anomalously high results when applied to waters rich in Mg^{++}. Figure 9 shows temperature corrections that should be subtracted from the Na-K-Ca calculated temperatures to correct for Mg^{++}. Temperature corrections also can be calculated using the following equations that were derived by Fournier and Potter (1979): For R between 5 and 50

$$\Delta t_{Mg} = 10.66 - 4.7415R + 325.87(\log R)^2 - 1.032\times10^5(\log R)^2/T - 1.968\times10^7(\log R)^2/T^2 + 1.605\times10^7(\log R)^3/T^2, \quad (11)$$

and for $R < 5$

$$\Delta t_{Mg} = -1.03 + 59.971\log R + 145.05(\log R)^2 - 36711(\log R)^2/T - 1.67\times10^7 \log R/T^2, \quad (12)$$

where

R = [Mg/(Mg + Ca + K)] x 100, with concentrations expressed in equivalents.

Δt_{Mg} = the temperature correction in °C that should be subtracted from the Na-K-Ca calculated temperature.

T = the Na-K-Ca calculated temperature in °K.

For some conditions, equations 11 and 12 may give negative values for Δt_{Mg}. In that event, do not apply a Mg^{++} correction to the Na-K-Ca geothermometer.

As with other geothermometers, the Mg-corrected Na-K-Ca geothermometer is subject to error owing to continued water-rock reaction as an ascending water cools. If the Mg^{++} concentration increases during that upward flow, application of an Mg^{++} correction will lead to an anomalously low calculated reservoir temperature. At this time there is no easy "rule of thumb" to determine when and when not to apply an Mg^{++} correction to the Na-K-Ca geothermometer. That decision should be based upon the general geologic and hydrologic setting of the particular water that was sampled. However, high magnesium concentrations do indicate that water-rock reactions have occured at relatively low temperatures. Therefore chemical geothermometer results should be used with great caution when applied to Mg-rich waters.

The $\Delta^{18}O$ ($SO_4^{=}$ - H_2O) Geothermometer

The sulfate oxygen isotope geothermometer is based upon the experimental work of Lloyd (1968), who measured the exchange of ^{16}O and ^{18}O between $SO_4^{=}$ and water at 350°C, and the work of Mizutani and Rafter (1969) and Mizutani (1972) who measured the exchange of ^{16}O and ^{18}O between H_2O and HSO_4^{-} at 100-200°C. The agreement of the 100-200°C HSO_4^{-} data and the 350°C $SO_4^{=}$ data and other arguments suggest no fractionation of ^{16}O and ^{18}O between $SO_4^{=}$ and HSO_4^{-}. At the pH of most natural fluids SO_4^{-} is present rather than HSO_4^{-}.

The rate of equilibration was measured by Lloyd (1968). In the pH range of most deep geothermal waters, the rates of the sulfate oxygen isotope exchange reaction are very slow compared to silica solubility and cation exchange reactions. This can be advantageous for geothermometry because once equilibrium is attained after prolonged residence time in a reservoir at high temperature, there is little re-equilibration of the oxygen isotopes of sulfate as the water cools during movement to the surface, unless that movement is very slow. Unfortunately, if steam separation occurs during cooling, the oxygen isotopic composition of water will change. The fractionation of ^{16}O and ^{18}O between liquid water and steam is temperature dependent and comes to equilibrium almost immediately at temperatures as low as 100°C. Therefore, if a water cools adiabatically from a high temperature to 100°C, the liquid water remaining at the termination of boiling will have a different isotopic composition depending on whether steam escaped continuously over a range of temperatures or whether all the steam remained in contact with the liquid and separated at the final temperature, 100°C (Truesdell et al., 1977).

Although boiling makes interpretation more complex, it does not preclude use of the $\Delta^{18}O$ ($SO_4^{=}$ - H_2O) geothermometer. McKenzie and Truesdell (1977) showed that sulfate/oxygen isotope geothermometer temperatures could be calculated for three end-member models: (1) conductive cooling, (2) one step steam loss at any specified temperature, and (3) continuous steam loss. Where water is produced from a well and steam is separated at a known temperature (or pressure), there is no ambiguity in regard to which model to use. Likewise, conductive cooling is assumed for springs that emerge well below boiling.

The validity of temperatures calculated by the $\Delta^{18}O$ ($SO_4^{=}$ - H_2O) method is adversely affected by mixing of different waters (generally hot and cold) unless corrections are made for changes in isotopic composition of both the sulfate and water that result from that mixing. Even if the cold component of the mixture contains no sulfate, calculated sulfate/oxygen isotope temperatures will be in error unless the isotopic composition of the water is corrected back to the composition of the water in the hot component prior to mixing. Examples of calculated corrections for boiling and mixing effects applied to waters from Yellowstone National Park and Long Valley, California, were given by McKenzie and Truesdell (1977) and by Fournier et al. (1979).

The formation of sulfate by oxidation of H_2S at low temperatures is a particularly difficult problem to deal with when applying the sulfate/oxygen isotope geothermometer. A small amount of low-temperature sulfate can cause a large error in the geothermometer result. If analytical data are available for only one or two springs, addition of sulfate by H_2S oxidation may go unnoticed unless pH values are abnormally low. Where analytical data are available for several springs and they all have the same Cl/SO_4 ratio, oxidation of H_2S is probably unimportant. When variations in Cl/SO_4 are found in hot spring waters from a given region, the water with the highest Cl/SO_4 ratio has the best chance of being unaffected by H_2S oxidation.

UNDERGROUND MIXING OF HOT AND COLD WATERS

Recognition of Mixed Waters

Mixing of ascending hot water with cold groundwater in shallow parts of hydrothermal systems appears to be common. Mixing can also occur deep in hydrothermal systems, especially at the margins. The effects of mixing upon various geothermometers have been discussed previously.

Where all the thermal waters reaching the surface at a given locality are mixtures of hot and cold water, recognition of that situation can be difficult. The recognition that mixing took place underground is especially difficult where water-rock re-equilibration occurred after mixing. Complete or partial chemical re-equilibration is more likely if the temperature after mixing is well above 110°C to 150°C or if mixing takes place in aquifers with long fluid residence times.

Some indications of mixing discussed in Fournier (1979b) are as follows: (1) variations in chloride concentration of boiling springs too great to be explained by steam loss; (2) variations in ratios of relatively conservative elements that do not precipitate from solution during movement of water through rock, such as Cl/B; (3) variations in oxygen and hydrogen isotopes (especially tritium); (4) cool springs with large mass flow rates and much higher temperatures indicated by chemical geothermometers (greater than 50°C); (5) systematic variations of spring compositions and measured temperatures. Generally the colder water will be more dilute than the hotter water. However, in some situations the cold water component could be more concentrated than the hot water, such as where ocean water or closed-basin saline lake water mixes with an ascending hot water. The above indications of mixing may be shown by different compositions of nearby springs or by seasonal variations in a single spring.

The Silica Mixing Model

Under some circumstances the dissolved silica concentration of a mixed water may be used to determine the temperature of the hot water component (Fournier and Truesdell, 1974; Truesdell and Fournier, 1977). The simplest method of calculation uses a plot of dissolved silica *vs.* enthalpy of liquid water (figure 10). Although temperature is a measured property and enthalpy is a derived property, obtained from steam tables if temperature, pressure and salinity are known (Keenan *et al.*, 1969; Haas, 1976), enthalpy is used as a coordinate rather than temperature. This is because the combined heat contents of two waters at different temperatures are conserved when those waters are mixed (neglecting small heat of dilution effects), but the combined temperatures are not.

For most situations, solutions are sufficiently dilute so that enthalpies of pure water can be used to construct enthalpy-composition diagrams. A straight line drawn from a point representing the non-thermal component of the mixed water (point A, figure 10) through the mixed-water warm spring (point B) to the intersection with the quartz solubility curve gives the initial silica

concentration and enthalpy of the hot-water component (point C). This procedure assumes that any steam that formed adiabatically as the hot-water component moved up to a more shallow environment did not separate from the residual liquid water before mixing with the cold-water component.

Truesdell and Fournier (1977) discussed the procedure for determining the enthalpy and temperature of the hot water component when steam was lost before mixing took place. As an end-member assumption, consider that steam was lost at atmospheric pressure prior to mixing (point D, figure 10). The horizontal line drawn from point D to the intersection with the maximum steam loss curve gives the initial enthalpy of the hot-water component (point E). If steam had been lost at a higher pressure before mixing, point D would lie above 419 J/g on the extension of line AB and point E would lie at an appropriate dstance between the maximum steam loss and quartz solubility curves.

In order for the above silica mixing model to give accurate results, it is vital that no conductive cooling occurred after mixing. If the mixed water cooled conductively after mixing, the calculated temperature of the hot-water component will be too high. It is also necessary that no silica deposition occurred before or after mixing and that quartz controlled the solubility of silica in the high-temperature water. Even with these restrictions the silica mixing model has been found to give good results in many places. In special circumstances, a silica mixing model could be used in which chalcēdony or another silica phase is assumed to control the dissolved silica in the high-temperature component.

EFFECTS OF UNDERGROUND BOILING

An upflowing hot solution may boil because of decreasing hydrostatic head. If the rate of upflow is fast enough, cooling of the fluid may be approximately adiabatic. Where boiling occurs there is a partitioning of dissolved elements between the steam and residual liquid; dissolved gases and other relatively volatile components concentrate in the steam and non-volatile components become concentrated in the liquid in proportion to the amount of steam that separates. In a boiling process that takes place owing to a decrease in pressure from P_1 to P_2, Truesdell et al. (1977) showed that slightly different amounts of residual liquid water will remain at the end of the process depending upon whether the steam that forms is continuously removed from the system as pressure decreases, or whether the steam maintains contact and re-equilibrates with the cooling water until the steam is removed all at once at P_2 (single-stage steam loss). This distinction between processes involving continuous steam loss and single-stage steam loss is very important when dealing with volatile subtances (gases, isotopes), but can be neglected when dealing with non-volatile components.

Calculation of change in concentration resulting from boiling

For non-volatile components that remain with the residual liquid as steam separates, the final concentration, C_f, after single-stage steam separation at a given temperature, t_f, is given by the formula

$$C_f = \frac{(H_s - H_f)}{(H_s - H_i)} C_i \qquad (13)$$

where C_i is the initial concentration before boiling, H_i is the enthalpy of the initial liquid before boiling and H_f and H_s are the enthalpies of the final liquid and steam at t_f. For solutions with salinities less than about 10,000 mg/kg, enthalpies of pure water tabulated in steam tables (Keenan et al., 1969) can be used to solve equation (13). For higher salinities enthalpies of NaCl solutions can be used, such as those tabulated by Haas (1976). Equation (13) also can be solved graphically using a plot of enthalpy vs. a non-reactive dissolved constituent (such as chloride), as shown in figure 11. One-step steam loss processes can be represented by straight lines radial to the composition and enthalpy of steam in figure 11. Thus, if the enthalpy and concentrations of constituent x are known prior to boiling (point A in figure 11), the concentrations of x in the residual liquid after boiling can be obtained by extending a straight line from the enthalpy of steam at the final steam separation temperature through point A to the enthalpy of the remaining liquid water after boiling. For example, in figure 11, the initial condition at point A is 300°C and 100 units of x, the final steam separation takes place at 100°C, and point B gives the concentration of x in the residual liquid after steam separation. If final steam separation took place at 200°C, point C would give the concentration of x in the residual liquid. The process can be looked at in reverse. If the final concentration of x is known after steam separation at a given temperature, the initial concentration of x in the non-boiled solution can be determined graphically if the initial enthalpy is known; or, the initial enthalpy can be determined if the initial concentration of x is known.

Use of Enthalpy-chloride diagrams for estimating reservoir temperatures

Where a range in chloride concentration of hot springs appears to result mainly from different amounts of boiling, that range in concentration can give information about the minimum temperature of the reservoir feeding the springs (W. A. J. Mahon in Lloyd, 1972; Truesdell and Fournier, 1976b; Fournier, 1979b). For example, figure 12 shows the chloride range in two chemically distinct types of hot spring waters from Upper Basin in Yellowstone National Park, plotted at the enthalpies corresponding to liquid water at the measured temperature of each spring. The Geyser Hill type waters have ratios of $Cl/(HCO_3+CO_3)$, expressed in equivalents, greater than four and chloride concentrations ranging from 352 to 465 mg/kg. The Black Sand-type waters have $Cl/(HCO_3 + CO_3)$ ratios close to 0.9 and chlorides ranging from 242 to 312 mg/kg. The minimum temperature of the water in the reservoir feeding the Geyser Hill hot springs can be determined by first drawing a straight line from the spring with maximum chloride (point A) to the enthalpy of steam at 100°C, and then extending a vertical line from the spring with least chloride (point B). The intersection of that vertical line with the previous line, point C, gives the minimum enthalpy of the water in the reservoir, 936 joules, which indicates a temperature of 218°C (Keenan et al., 1969). The silica (quartz) geothermometer applied to water A (assuming maximum steam loss) gave a calculated reservoir temperature of 216°C and applied to water B (assuming no steam loss) gave a temperature of 217°C. The agreement between the calculated reservoir temperatures using silica and chloride relations is strong evidence that the reservoir feeding Geyser Hill has a temperature close to 218°C. The range in chloride concentrations in the Black Sand-type waters, E to D, suggests a reservoir temperature of about 209°C (point F in figure 12); the silica geothermometer gave 205°C.

Although point F in figure 12 represents a more dilute and slightly cooler water than point C, water F cannot be derived from water C by simple mixing of hot and cold water (point N) because any mixture would lie on or close to the line CN. Waters C and F are probably both related to a still higher enthalpy water such as G or H. Water F could be related either to water G or H by mixing in different proportions with N. Water C would be related to G by boiling (adiabatic cooling resulting from a decrease in hydrostatic head) and evaporative concentration of chloride in an ascending solution. Water C would be related to H by conductive cooling of a slow moving solution. The route G to C appears more likely because boiling and loss of CO_2 into the steam phase can explain the different $Cl/(HCO_3 + CO_3)$ ratios found in waters C and F. Using additional hot spring data from Midway and Lower Basins, Fournier et al. (1976) concluded that a reservoir at about 270°C underlies the Upper and Lower Basins and that a still hotter reservoir exists at greater depth.

Effect of boiling upon geochemical thermometers

The effect of underground boiling owing to decreasing hydrostatic head upon different geothermometers was covered previously as each geothermometer was discussed. In brief, adiabatic cooling affects different geothermometers in various ways: the Na/K geothermometer is not affected; the Na-K-Ca

geothermometer is significantly affected only if loss of CO_2 causes $CaCO_3$ to precipitate, resulting in calculated temperatures that are too high; the silica geothermometer must be corrected for separation of steam; and the $\Delta^{18}O(SO_4^{=} - H_2O)$ geothermometer also must be corrected for steam loss because of the temperature-dependent fractionation of oxygen isotopes between liquid water and steam.

VAPOR-DOMINATED COMPARED TO HOT WATER SYSTEMS

The model of a vapor-dominated system formulated by White et al. (1971) is now generally accepted. In that model, relatively impermeable rock and locally derived shallow groundwater provide a cap over a reservoir of considerable vertical extent in which steam is the continuous phase in relatively open channelways and liquid water fills most of the intergranular pore spaces (figure 13). Fluid temperature and pressure increase with increasing depth above the steam zone. Within the steam zone, fluid pressure remains relatively constant because steam weighs very little compared to water, so there is little change in hydrostatic head. Temperature also is relatively constant throughout the steam zone because the temperature of a mixture of steam and water depends on pressure. Below the steam zone, liquid fills the open channels and pressures and temperatures again increase with increasing depth. In contrast, in a hot-water system, hot water is the continuous phase in the open channels, although bubbles of steam or gas may be present in the water (figure 14). Hydrostatic pressure continuously increases with depth, and the maximum temperature is limited by a boiling point curve (Haas, 1971).

Where a vapor-dominated system is present, it is likely that steam carrying relatively volatile components such as NH_3, CO_2, H_2S, Hg and B will condense in the overlying cap-rock region. The slightly volatile components will redissolve in the condensate, but some of the more volatile components are likely to continue moving up into overlying colder groundwater. Thus, groundwaters and springs over vapor-dominated systems tend to be rich in the above mentioned volatile components of the geothermal fluid or their reaction products and low in non-volatile components, such as chloride, which remain in the residual brine at depth.

Fumaroles, mud pots, acid-sulfate springs with low rates of discharge, sodium bicarbonate spring waters, and acid-altered hot ground are typical surface expressions of vapor-dominated systems. They are not unique to vapor-dominated systems, however, because similar features commonly are present over hot-water systems where underground boiling occurs. Generally, but not always, chloride-rich neutral to alkaline springs emerge above hot-water systems at topographically low places and acid sulfate springs and mud pots emerge at higher elevations. The Coso, California, geothermal area is an example of a situation where the surface expression of a hot water-dominated system consists only of low-chloride, acid sulfate springs and other features typically equated with vapor-dominated systems. Drilling at Coso Hot Springs showed that a chloride-rich, hot-water system exists at depth with the top of the hot water reaching to within 30 to 45 meters of the ground surface (Fournier et al., 1980; Austin and Pringle, 1970).

COMPARISON OF THERMAL WATERS FROM SPRINGS AND WELLS

Chemical analyses of representative waters from wells and springs at various geothermal localities are listed in table 2.

The enthalpy-chloride diagrams shown in figure 15 were drawn using data from table 2 and assuming cold water components with relatively little chloride and temperatures ranging from 4° to 20°C, depending on latitude and elevation of the geothermal field. Enthalpies of the solutions at known temperatures and salinities were obtained from steam tables (Keenan et al., 1969; Haas, 1976) assuming liquids at the vapor pressure of the solution at the given temperatures and no excess steam. In figure 15a, point 26 (Spring 664) from Orakeikorako, N. Z. lies very close to the straight line extending from the deep hot water component, point 24, to the cold water component. Therefore, it appears there was little conductive cooling after mixing. This is consistant with the relatively high rate of mass flow of Spring 664, 12 L/sec. When additional hot spring data (W. A. J. Mahon in Lloyd, 1972) are employed in the interpretation, it appears that water from a lower temperature aquifer (~180° to 240°C), such as point P in figure 15a, probably mixes with cold waters to give point 26 (Fournier, 1979b). This conclusion is also supported by the relatively low Na/K temperature of 194°C for water in column 26.

In figure 15b the three Cerro Prieto springs all lie below the line drawn from cold water to the high-temperature deep water, point 13. It is very likely that number 14 cooled by conduction from a temperature near 200°C after mixing. The alkalies in that mixed water have retained the high-temperature imprint of the deep hot-water component but silica has precipitated. Samples 15 and 16 also appear to have cooled by conduction after mixing, but either sample could result by mixing cold water with a hot water from a reservoir with a temperature below 290°C. Alkali geothermometers applied to the mixed waters give temperatures significantly lower than 290°C, indicating considerable water-rock reactions that could have occured in reservoirs with intermediate temperatures.

Hot spring 181 from El Tatio, Chili, point 3 in figure 15c, emerges at the boiling temperature for the elevation. That mixed water could have cooled by conduction, adiabatically, or a combination of these processes. The salinity and maximum enthalpy of the water just after mixing should lie between the points a and b.

The two springs from Ahuachapán, points 7 and 8 in figure 15d, both lie above the mixing line of cold water with deep water. Their position above the line could result (a) from mixing with a high-temperature component having much higher enthalpy than point 6 or (b) from condensation of excess steam derived from boiling water at depth (distillation). Excess steam appears to be the more plausible explanation because the spring waters are relatively rich in volatile components, $SO_4^=$ and HCO_3^-.

In summary, based on the chloride concentrations in spring waters compared to chloride concentrations at depth and in flashed well waters, springs in columns 3, 11, 42, and 45 appear to have cooled mainly adiabatically, springs in columns 22, 25 and 39 partly adiabatically and partly by conduction, and the spring in column 19 by conduction. Based on boron and other dissolved constituents, spring 32 also cooled conductively. The rest of the springs appear to be mixed waters.

The direct application of chemical geothermometers to the spring waters listed in table 2 gives variable results as shown in figure 16. Chemical geothermometers applied to some of those hot spring waters give accurate indications of reservoir temperatures encountered in drill holes, but most give lower temperatures. However, the results shown in figure 16 are somewhat misleading because in many places reservoirs at intermediate temperatures are present but have been cased off in an attempt to produce only from deeper and higher-temperature parts of the system.

The main generalization that can be drawn from a comparison of the well and spring data shown in table 2 is that waters tend to react chemically with wall rocks after the waters leave deep reservoirs and before emerging at the surface. These reactions may take place in intermediate reservoirs or in the channelways leading to the surface. As temperatures decrease, both HCO_3^- and $SO_4^=$ commonly increase, K^+ decreases relative to Na^+, and Ca^{++} increases relative to Na^+ unless $CaCO_3$ precipitates. The Mg^{++} data are incomplete, but in some places, such as Cerro Prieto and Reykjanes, there are very significant increases in Mg^{++} in the spring waters compared to the deep waters. This increase in Mg^{++} as hot waters cool leads to a dilemma in the application of the Mg correction for the Na-K-Ca geothermometer devised by Fournier and Potter (1979). Waters which were never very hot may give Na-K-Ca temperatures which are much too high unless an Mg^{++} correction is applied. On the other hand, waters which start out hot and react with wall rocks as they cool may give Na-K-Ca temperatures which are closer to the temperature deep in the system than the Mg^{++} corrected temperatures.

Continued water-rock reactions as solutions move up from depth and cool are not always a detriment in regard to obtaining useful information about a given hydrothermal system. The geographic distribution of springs with different water compositions and different gas contents may show directions of underground hot water movement (Truesdell, 1976b) as well as successive chemical re-equilibrations at lower temperatures.

APPLICATIONS FOR RESERVOIR ENGINEERING

Geochemistry has many applications for reservoir engineering. It provides information about noncondensable gases that decrease turbine efficiency, environmental concerns in regard to waste disposal, and scaling and corrosion associated with production and reinjection. Illustrations of a few other applications are given below.

Early Indication of Aquifer Temperatures in Wells

Geochemical thermometers may be used to estimate aquifer temperatures in wells weeks or months before underground temperatures return to normal after drilling. Flow testing may speed the temperature recovery in the production zone, but interferes with obtaining information about pre-drilling temperatures elsewhere in the well. Also, extensive flow testing immediately after the termination of drilling is not always possible because of limited brine containment or disposal facilities or delayed delivery of test equipment. Production and collection of a small amount of fluid at the wellhead or a downhole water sample, however, may be all that is necessary to provide a good indication of the aquifer temperature.

A 1477 m geothermal exploration well (CGEH No. 1) was drilled near Coso Hot Springs, California, in 1977 (Goranson and Schroeder, 1978). The same day that the well was completed, it was stimulated into production for 1 hour at a rate of 29 to 36 m^3/hr using an air lift. Water samples were collected for chemical analyses every 15 minutes during that production. The Na-K-Ca geothermometer applied to those waters ranged from 191°C at the start to 194°C at the end of the production period, and the Na/K geothermometer gave 195°C to 198°C (Fournier et al., 1980). Before stimulation the maximum temperature in the well was 165°C, and six days after stimulation the maximum temperature was 178°C. After 3 months the maximum temperature in the quiescent well had increased to 187°C, and after 4 months, it was 195°C. It is significant that the first water collected from the well immediately after well completion gave a good indication of the reservoir temperature even though about 1.3×10^6 L of makeup water and 1.3×10^5 kg dry weight of mud were injected into the formation during drilling.

Monitoring Temperature Changes in Production Wells

It is expensive to interrupt production of a geothermal well to run a temperature log. Logging a well is also a relatively slow process, and a temperature survey of a field with several production wells could take many days or weeks. By the time the last well is logged the temperatures in the first wells could have changed. To overcome these disadvantages Mahon (1966) devised a method of monitoring temperatures of waters supplying drillholes at Wairakei using the silica content of that water. Water samples could be collected from all the producing wells the same day without interrupting production. Calculated temperatures were within ±3°C of downhole measured temperatures which in turn were good only to ±3°C. Mahon (1966) also showed that the silica concentration in the water entering wells did decrease in response to decreasing temperatures of the aquifer.

Confirmation of Production from Multiple Aquifers at Different Temperatures

Mercado (1970) found that variations in the Na/K ratio in well waters at Cerro Prieto, Mexico were very useful for interpreting well behavior. He discussed well M-20 in detail. Upon completion of that well, water started flowing spontaneously through a small 1.27-cm diameter drain line. Subsequently the rate of discharge was periodically increased by allowing the fluid to escape through larger and larger orifice plates up to 14.6 cm diameter. As the orifice plate diameter was increased, the enthalpy of the discharge decreased and the Na/K ratio in the discharged fluid increased. The variations in the Na/K ratio clearly showed that more than one aquifer supplied water to the well and that the proportion of water from the cooler aquifers increased as the total rate of production from the well was allowed to increase (and downhole pressure decrease).

Variations in the chloride concentration of the produced fluid also can give a good indication of production from different aquifers.

Flashing in the Reservoir

Drawdown can cause flashing or boiling in the reservoir before the liquid enters the well. Flashing in the reservoir can result in enthalpies of the discharged fluid that are higher or lower than the initial enthalpy of the liquid in that reservoir.

Where a flashing front moves out into rock away from a well and the fluid pressure in the formation drops below the initial vapor pressure of the solution, the fluid temperature will decrease almost immediately owing to vaporization of liquid. Rock temperatures, however, do not decrease as rapidly as fluid temperatures. Transfer of heat from the reservoir rock to the fluid will cause more steam to form than would form by simple adiabatic expansion of the fluid. If this "excess" steam enters the well along with the residual liquid, the enthalpy of the discharged fluid will be higher than the enthalpy of the initial fluid in the reservoir. "Excess" steam has been described in fluids produced from wells at Wairakei and Broadlands, New Zealand (Grindley, 1965; Mahon and Finlayson, 1972) and at Cerro Prieto, Mexico (Truesdell and Mañon, in press).

A relatively low enthalpy of the discharged fluid will result if some or all of the steam fails to enter the well along with the parent water. The steam may escape upward through porous rock or may form a steam cap above the inlet to the well. Where a steam cap forms, enlargement of the steam zone could cause wells to switch eventually from producing fluids with relatively low enthalpy to producing fluids with relatively high enthalpy or even dry steam.

From the foregoing discussion it follows that reservoir temperatures based upon wellhead enthalpy measurements may be too high or too low even where only one aquifer contributes fluid to the well. The application of geochemistry may indicate whether or not flashing is occurring in the reservoir and whether excess or deficient steam accompanies the produced liquid.

Truesdell and Mañon (in press) used the silica concentration in flashed (atmospheric pressure) well waters at Cerro Prieto, Mexico to detect excess and deficient steam in the produced fluids. They calculated aquifer temperatures using the silica geothermometer and compared those results with aquifer temperatures calculated from measured enthalpies of the discharged fluids. A higher calculated reservoir temperature, based upon silica, indicates boiling with steam segregation in the formation and liquid water preferentially produced into the well. A calculated reservoir temperature, based upon silica, that is lower than the reservoir temperature based upon enthalpy also suggests boiling in the formation, but excess steam enters the well owing to boiling caused by heat stored in the reservoir rock. The situation is somewhat ambiguous, however, because a relatively low calculated silica temperature also would result if silica precipitated before the water sample was collected for analysis. Even in the absence of silica precipitation in the formation or well, another difficulty is that the silica-enthalpy method might not indicate an outward migrating flashing front unless there is segregation of steam and residual liquid in the formation; without segregation both the silica and enthalpy of the produced fluid will indicate about the same aquifer temperature that is higher than the actual temperature. In some places the above difficulties can be overcome by using the Na/K geothermometer instead of the silica geothermometer (Truesdell et al., 1979).

Another approach is to use Na/K geothermometer temperatures in conjunction with silica and enthalpy temperatures to do a better job of evaluating flashing in the formation (Truesdell et al., 1979). Aquifer temperatures calculated independently from silica, Na/K, and enthalpy of the produced fluid can all be in agreement (no indication of flashing in the reservoir), be in partial agreement, or all be different. There are 13 possible combinations of results. Some of the most likely combinations can be interpreted as follows:

Where silica and Na/K temperatures are in near agreement and either higher or lower than the enthalpy temperature, it is likely that the enthalpy temperature is in error owing to flashing in the formation with a disproportionate amount of steam entering the well. Where Na/K and enthalpy agree and silica gives a lower temperature, silica probably precipitated before the sample was collected. Where silica and enthalpy agree and Na/K gives a lower temperature, there may be an outward moving flashing front in the formation without segregation of steam and residual liquid that enter the well.

Where silica and enthalpy agree and Na/K gives a higher temperature, the Na/K value may be residual from a time when the water equilibrated with rock at a higher temperature than that which is present in the immediate aquifer supplying fluid to the well. There are indications at Wairakei and Broadlands, New Zealand, that Na/K does not respond as rapidly as silica to a change in underground temperature (Ellis and Mahon, 1977).

Evidence of Higher Temperatures Elsewhere within a System

A comparison of the composition of wellhead and downhole water samples may help verify the existence of a deeper and higher-temperature reservoir than that indicated by temperature measurements in a well. An example is at Coso Hot Springs, California, where a shallow 114 m prospect geothermal well was drilled by the U. S. Navy in June 1967. In March 1968, the well was produced by bailing after the bottom hole temperatures had stabilized at 142°C (Austin and Pringle, 1970). A wellhead sample collected toward the end of the bailing activity contained 3042 mg/kg chloride after flashing at atmospheric pressure. Cation geothermometer temperatures applied to that water indicated a reservoir temperature of about 240°C to 250°C. Figure 17 shows enthalpy-chloride relations that could yield the wellhead sample, point A. Point B represents the condition of the water at the bottom of the well at 142°C, assuming maximum adiabatic cooling during bailing. The water flowing into the well in response to the bailing could have moved up quickly from the high-temperature reservoir, boiling as it came with little conductive heat loss (route CBA) or it could have cooled entirely conductively before entering the well (route DBA). Line CD shows the probable range in chloride concentration in the deep reservoir, assuming that the reservoir temperature is between 240°C and 250°C and cooling is partly adiabatic and partly conductive. In 1978 a downhole sample was obtained and analyzed (Fournier, et al., 1980). The chloride was 2370 mg/kg and geothermometer temperatures were Na-K-Ca = 234°, Na/K = 231°, and $\Delta^{18}O(SO_4=-H_2O)$ = 243°C. In figure 17 point E shows the condition of the downhole sample at the point of collection and point F gives the calculated condition according to the geothermometers. The difference in chloride between the wellhead sample after flashing (point A) and without flashing (point E) indicates that flashing occurred in the formation in response to the bailing and that the minimum temperature in the reservoir supplying water to the well should be at least 215°C. The near agreement of all the geothermometer temperatures applied to the wellhead and downhole samples strongly suggests that the actual temperature of the reservoir supplying water to the well is near 240°C and water from that reservoir cooled partly adiabatically and partly by conduction when the well was bailed.

Geochemical Evidence of Drawdown

In a vapor-dominated system, the movement of recharge water into the production zone as a result of drawdown may be advantageous for the efficient extraction of heat stored in the rock without significantly lowering the reservoir temperature and pressure. In hot-water systems, however, the rapid influx of surrounding cold water or reinjected waste water may significantly lower the temperature of the produced fluid in a few years. Where there is an influx of cold water into the production zone, Nathenson (1975) showed that chemical changes should precede thermal changes and that the elapsed time between these changes is related to the porosity of the rock. With 0.2 porosity, chemical changes that appear X years after the start of production indicate that thermal changes will appear about 3.4 X years later.

At Larderello, Italy, the movement of recharge water into the vapor-dominated system is indicated by the appearance of tritium in steam produced from wells at the margins of the production zone (Celati et al., 1973). In the hot-water system at Cerro Prieto, Mexico, drawdown of fluids from an overlying lower-temperature aquifer is shown in the southeastern part of the field by a decrease in the chloride concentration in well water and an increase in the Na/K ratio (Truesdell et al., 1979).

SUMMARY

The ratios of the cations in geothermal fluids are controlled by temperature-dependent water-rock reactions with chemical equilibrium attained in high-temperature reservoirs where fluid residence times are relatively long (years).

At present the most useful geochemical thermometers or geothermometers are silica, Na/K, Na-K-Ca, and $\Delta^{18}O(SO_4^{=} - H_2O)$. Each of these geothermometers requires special consideration in its application. In many places, some or all of these geothermometers applied to hot spring waters give good indications of deep reservoir temperature. In other places, however, these geothermometers give information only about shallow reservoirs containing more dilute and lower-temperature fluids than are present in deeper reservoirs. Under some conditions mixing models may be used to estimate reservoir temperatures and salinities in deeper reservoirs than is otherwise possible.

Geochemistry can be used to estimate reservoir temperatures encountered by newly drilled wells long before temperature logs give a good indication of predrilling conditions. Geochemistry can also be a powerful and sensitive tool for detecting changes in a reservoir during production, particularly when used in conjunction with physical measurements at the wellhead.

REFERENCES

Arnórsson, S. (1975). "Application of the silica geothermometer in low temperature hydrothermal areas in Iceland," Am. J. Sci., 275, 763-784.

Arnórsson, S. (1978). "Major element chemistry of the geothermal sea-water at Reykjanes and Svartsevgi, Iceland," Miner. Mag., 42, 209-220.

Austin, C. F., and Pringle, J. K. (1970). "Geologic investigations at the Coso Thermal Area," Naval Weapons Center Technical Publication 4878, 40 p.

Bargar, K. E., Beeson, M. H., Fournier, R. O., and Muffler, L. J. P. (1973). "Present-day lepidolite from thermal waters in Yellowstone National Park," Amer. Mineral., 58, 901-904.

Björnsson, S., Arnórsson, S., and Tómasson, J. (1972). "Economic evaluation of Reykjanes thermal brine area, Iceland," Amer. Assoc. Petroleum Geologists Bull., 56, 2380-2391.

Bodvarsson, G. (1960). "Exploration and exploitation of natural heat in Iceland," Bull. Volcanol., 23, 241-250.

Browne, P. R. L. (1978). "Hydrothermal alteration in active geothermal fields," Annual Review in Earth and Planetary Sciences, 6, 229-250.

Browne, P. R. L. and Ellis, A. J. (1970). "The Ohaki-Broadlands hydrothermal area, New Zealand, mineralogy and related geochemistry, Amer. J. Sci. 269, 97-131.

Busey, R. H., and Mesmer, R. E. (1977). "Ionization equilibria of silicic acid and polysilicate formation in aqueous sodium chloride solutions to 300°C," Inorg. Chem., 16, 2444-2450.

Celati, R., Noto, P., Panichi, C., Squarci, P. and Taffi, L. (1973). "Interactions between the steam reservoir and surrounding aquifers in the Larderello Geothermal Field", Geothermics, 2(3-4), 174-185.

Cusicanqui, H., Mahon, W. A. J., and Ellis, A. J. (1976). "The geochemistry of the El Tatio geothermal field, Northern Chile," Second United Nations Symposium on the Development and Use of Geothermal Resources, San Francisco, May, 1975, 1, 703-711.

Dominco, E. and Şâmilgil, E. (1970). "The geochemistry of the Kizildere geothermal field, in the framework of the Saraykey-Denizli geothermal area," United Nations Symposium on the Development and Utilization of Geothermal Resources, Pisa, 1970, 2, part 1, 553-560.

Ellis, A. J. (1966). Volcanic hydrothermal areas and the interpretation of thermal water compositions," Bull. Volcanologique, 29, 575-584.

Ellis, A. J. (1969). Present-day hydrothermal systems and mineral deposition: Proceedings, Ninth Commonwealth Mining and Metallurgical Congress, Mining and Petroleum Geology Section, The Inst. of Mining and Metallurgy, London, p. 1-30.

Ellis, A. J. (1970). "Quantitative interpretation of chemical characteristics of hydrothermal systems," Geothermics, Special Issue 2, 2(1), 516-528.

Ellis, A. J., and Mahon, W. A. J. (1967). "Natural hydrothermal systems and experimental hot-water/rock interactions (Part 2)," Geochim. Cosmochim. Acta, 31, 519-539.

Ellis, A. J., and Mahon, W. A. J. (1977). Chemistry and Geothermal Systems, Academic Press, New York, 392 pp.

Fournier, R. O. (1973). "Silica in thermal waters: Laboratory and Field investigations," Proceedings of International Symposium on Hydrogeochemistry and Biogeochemistry, Japan 1970, Volume 1, Hydrogeochemistry: Washington, D.C., J. W. Clark, 122-139.

Fournier, R. O. (1977). "Chemical geothermometers and mixing models for geothermal systems," Geothermics, 5, 41-40.

Fournier, R. O. (1979a). "A revised equation for the Na/K geothermometer." Geothermal Resources Council Transactions, 3, p. 221-224.

Fournier, R. O. (1979b). "Geochemical and hydrologic considerations and the use of enthalpy-chloride diagrams in the prediction of underground conditions in hot spring systems," J. Volcanol. Geotherm. Res. 5, 1-16.

Fournier, R. O., and Potter, R. W. II (1979). "Magnesium correction to the Na-K-Ca chemical geothermometer," Geochim. Cosmochim. Acta, 43, P. 1543-1550.

Fournier, R. O., and Rowe, J. J. (1966). "Estimation of underground temperatures from the silica content of water from hot springs and wet-steam wells," Am. J. Sci., 264, 685-697.

Fournier, R. O., Sorey, M. L., Mariner, R. H., and Truesdell, A. H. (1979). "Chemical and isotopic prediction of aquifer temperatures in the geothermal system at Long Valley, California," J. Volcanol. Geothermal Res. 5, 17-34.

Fournier, R. O., Thompson, J. M., and Austin, C. F. (1980). Interpretation of chemical analyses of waters collected from two geothermal wells at Coso, California," J. Geophys. Res. 85, p. 2405-2410.

Fournier, R. O., and Truesdell, A. H. (1970). "Chemical indicators of subsurface temperature applied to hot spring waters of Yellowstone National Park, Wyoming U.S.A.," Geothermics, Special Issue 2, 2(1) 529-535.

Fournier, R. O., and Truesdell, A. H. (1973). "An empirical Na-K-Ca geothermometer for natural waters," Geochim. Cosmochim. Acta, 37, 1255-1275.

Fournier, R. O., and Truesdell, A. H. (1974). "Geochemical indicators of subsurface temperature--Part 2, estimation of temperature and fraction of hot water mixed with cold water," J. Res. U. S. Geol. Survey, 2, 263-270.

Fournier, R. O., White, D. E., and Truesdell, A. H. (1976) Convective heat flow in Yellowstone National Park," Second United Nations Symposium on the Development and Use of Geothermal Resources, San Francisco, May, 1975, 1, 731-739.

Goranson, C., and Schroeder, R. (1978). "Static downhole characteristics of well CGEH-1 at Coso Hot Springs, China Lake, California," Lawrence Berkeley Laboratory Report LBL-7059, 27 p.

Grindley, G. W. (1965). "The geology, structure, and exploitation of the Wairakei geothermal field, Taupo, New Zealand," New Zealand Geol. Survey Bull. 75, 131 p.

Haas, J. L., Jr. (1971). "Effect of salinity on the maximum thermal gradient of a hydrothermal system at hydrostatic pressure," Econ. Geol. 66, 940-946.

Haas, J. L., Jr. (1976). "Thermodynamic properties of the coexisting phases and thermochemical properties of the NaCl component in boiling NaCl solutions," U. S. Geol. Survey Bull. 1421-8, 71 p.

Helgeson, H. C. (1969). "Thermodynamics of hydrothermal systems at elevated temperatures and pressures," Am. J. Sci., 267, 729-804.

Helgeson, H. C., Brown, T. H., and Leeper, R. H. (1969). Handbook of Theoretical Activity Diagrams Depicting Chemical Equilibria in Geological Systems Involving an Aqueous Phase at One Atm and 0° to 300°C, Cooper, San Francisco, 253 p.

Keenan, J. H., Keyes, F. G., Hill, P. G., and Moore, J. G. (1969). Steam Tables (International Edition - Metric Units), Wiley, New York, 162 p.

Kennedy, G. C. (1950). "A portion of the system silica-water," Econ. Geol. 45, 629-653.

Kharaka, Y. K., and Barnes, Ivan (1973). "SOLMNEQ: Solution-mineral equilibrium computations," U.S. Geological Survey Computer Center, U.S. Department of Commerce, National Technical Information Service, Springfield, Virginia 22151, Report PB-215899, 82 p.

Lloyd, E. F. (1972). "Geology and hot springs of Orakeikorako," New Zealand Geol. Survey Bull. 85, 164 p.

Lloyd, R. M. (1968). "Oxygen isotope behavior in the sulfate-water system," J. Geophys. Res. 73(15), 6099-6110.

Mahon, W. A. J. (1966). Silica in hot water discharged from drillholes at Wairakei, New Zealand," New Zealand J. Sci. 9, 135-144.

Mahon, W. A. J., and Finlayson, J. B. (1972). "The chemistry of the Broadlands geothermal area, New Zealand," Am. J. Sci., 272, 48-68.

McKenzie, W. F., and Truesdell, A. H. (1977). "Geothermal reservoir temperatures estimated from the oxygen isotope compositions of dissolved sulfate and water from hot springs and shallow drillholes," Geothermics 5, 51-61.

Mercado G., S. (1968). "Localización de zonas de maxima actividad hidrotermal por medio de proporciones químicas. Campo geotérmico Cerro Prieto, Baja California, México," III Congreso Mexicano de Química Pura y Aplicada: Comisión Federal de Electricidad. Comisión de Energía Geotérmica, 32 pp.

Mercado G., S. (1970). "High activity hydrothermal zones detected by Na/K, Cerro Prieto, Mexico," Geothermics, Special Issue 2, 2(2) 1367-1376.

Mineral Research and Exploration Institute (No date). "Kizildere geothermal field in Turkey," Pamphlet published by the MTA, 12 pp.

Mining Research and Service Organization (1977), "Geothermal energy in Taiwan, Republic of China," MRSO (1977) Report-162, 10 p.

Mizutani, Y. (1972). "Isotopic composition and underground temperature of the Otake geothermal water, Kyushu, Japan," Geochem. J. (Japan), 6(2), 67-73.

Mizutani, Y. and Rafter, T.A. (1969). "Oxygen isotopic composition of sulphates—part 3. Oxygen isotopic fractionation in the bisulfate ion-water system. New Zealand J. Sci., 12(1), 54-59.

Morey, G. W., Fournier, R. O., and Rowe, J. J. (1962). "The solubility of quartz in water in the temperature interval from 29° to 300°C," Geochim. Cosmochim Acta 26, 1029-1043.

Morey, G. W., Fournier, R. O., and Rowe, J. J., , (1964). "The solubility of amorphous silica at 25°C," J. Geophys. Res, 69, 1995-2002.

Nathenson, Manuel (1975). "Physical factors determining the fraction of stored energy recoverable from hydrothermal convection systems and conduction dominated areas," U.S. Geological Survey Open-file Report 75-525, 51 p.

Reed, M. J. (1976). "Geology and hydrothermal metamorphism in the Cerro Prieto geothermal field, Mexico," Second United Nations Symposium on the Development and Use of Geothermal Resources, San Francisco, May, 1975, 1, 539-547.

Robie, R. A., Hemingway, B. S., and Fisher, J. R. (1978). "Thermodynamic properties of minerals and related substances at 298.15 K and one bar pressure and at higher temperatures," U.S. Geological Survey Bull. 1452, 456 p.

Romagnoli, P., Cuéllar, F., Jimenez, M., and Chezzi, G. (1976). "Aspectos Hidrogeológicos del Campo Geotérmico de Ahuachapán, El Salvador," Second United Nations Symposium on the Development and Use of Geothermal Resources, San Francisco, May, 1975, 1, 563-570.

Seward, T. M. (1974). "Determination of the first ionization constant of silicic acid from quartz solubility in borate buffer solutions to 350°C," Geochim. Cosmochim. Acta, 38, 1651-1664.

Truesdell, A. H. (1976a). "Summary of section III--geochemical techniques in exploration," Second United Nations Symposium on the Development and Use of Geothermal Resources, San Francisco, May, 1975, 1, liii-lxiii.

Truesdell, A. H., (1976b). "Chemical evidence of subsurface structure and flow in geothermal system," in, Proceedings Int. Symp. on Water-Rock Interaction, Czechoslovakia, 1974, p. 250-257.

Truesdell, A. H., and Fournier, R. O. (1976a). "Calculation of deep temperatures in geothermal systems from the chemistry of boiling spring waters of mixed origin," Second United Nations Symposium on the Development and Use of Geothermal Resources, San Francisco, May, 1975, 1, p. 837-844, U. S. Gov. Printing Office.

Truesdell, A. H. and Fournier, R. O. (1976b). "Conditions in the deeper parts of the hot spring systems of Yellowstone National Park, Wyoming," U.S. Geological Survey Open-File Report 76-428, 22 p.

Truesdell, A. H. and Fournier, R. O. (1977). "Procedure for estimating the temperature of a hot water component in a mixed water using a plot of dissolved silica versus enthalpy," J. Res. U.S. Geological Survey, 5(1), 49-52.

Truesdell, A. H., and Hulston, J. R. (1980). "Isotopic evidence on environments of geothermal systems," in, Fritz, P. and Fontes, J. C., Eds., Handbook of environmental isotope geochemistry, Volume 1: The terrestrial environment, Elsevier Press, Amsterdam, p. 170-225.

Truesdell, A. H., and Mañon, A. (in press). "Geochemical indications of boiling in the aquifer of The Cerro Prieto Geothermal field," Primera Reunión de Intercambio Técnico Sobre Geotérmia, San Filipe, B. C., 1977.

Truesdell, A. H., Mañon, A., Jimenez, M., Sanchez, A., and Fausto, J. (1979). "Geochemical evidence of drawdown in the Cerro Prieto, Mexico geothermal field," Symposium on the Cerro Prieto, Baja California, Mexico Geothermal Field, San Diego, September 1978. Lawrence Berkeley Laboratory Report LBL-7098, p. 130-138.

Truesdell, A. H., Nathenson, M., and Rye, R. O. (1977). "The effects of subsurface boiling and dilution on the isotopic compositions of Yellowstone thermal waters," J. Geophys. Res., 82(26), 3694-3703.

Truesdell, A. H., and Singers, W. (1974). "Computer calculation of down-hole chemistry in geothermal areas," U.S. Geological Survey J. Res., 2(3), 271-278.

Watson, J. C. (1978). "Sampling and analysis methods for geothermal fluids and gases," Battelle publication PNL-MA-572, UC-66d, available from NTIS, Springfield, Va.

White, D. E. (1965). "Saline waters of sedimentary rocks," Amer. Assoc. Petroleum Geologists, Mem. 4, p. 352-366.

White, D. E. (1970). "Geochemistry applied to the discovery, evaluation, and exploitation of geothermal energy resources," Geothermics, Special Issue 2, 1, 58-80.

White, D. E., Muffler, L. J. P., and Truesdell, A. H. (1971). "Vapor-dominated hydrothermal systems compared with hot-water systems," Econ. Geology, 66, 75-97.

Wildman, L. D., Jackson, M. L., and Whittig, L. D. (1968). "Serpentine rock dissolution as a function of carbon dioxide pressure in aqueous solution," Amer. Miner., 53, 1250-1263.

Figure Captions

Figure 1.--Phase diagram showing estimated stability fields for various minerals at different $[Na^+]/[H^+]$ and $[K^+]/[H^+]$ activity ratios in the presence of quartz at 260°C. Dashed lines show a portion of the diagram at 230°C (from Browne and Ellis, 1970).

Figure 2.--Phase diagram showing estimated stability fields for various minerals at different $[K^+]/[H^+]$ and $[Ca^{++}]/[H^+]^2$ activity ratios in the presence of quartz. Also shown are activity ratios of $[Ca^{++}]/[H^+]^2$ at which calcite will precipitate for $\underline{m}\ CO_2$ values of 0.01, 0.15, and 1.0 (from Ellis, 1969).

Figure 3.--Theoretical variation of $[Na^+]/[K^+]$ activity ratio in solutions equilibrated with alkali feldspar pairs with indicated structural states at 25°C to 300°C (data from Helgeson et al., 1969).

Figure 4.--Solubility of quartz (curve A) and amorphous silica (Curve C) as a function of temperature at the vapor pressure of the solution. Curve B shows the amount of silica that would be in solution after an initially quartz-saturated solution cooled adiabatically to 100°C without any precipitation of silica (from Fournier and Rowe, 1966, and Truesdell and Fournier, 1976a).

Figure 5.--Solubilities of various silica phases in water at the vapor pressure of the solution. A = amorphous silica, B = β-cristobalite, C = α-cristobalite, D = chalcedony, and E = quartz (from Fournier, 1973).

Figure 6.--Calculated effect of pH upon the solubility of quartz at various temperatures from 25°C to 350°C, using experimental data of Seward (1974). The dashed curve shows the pH required at various temperatures to achieve a 10 percent increase in quartz solubility compared to the solubility at pH 7.0.

Figure 7.--Na/K ratios of natural waters plotted at measured downhole temperatures in wells. Curve A is the least-squares fit of the data points above 80°C. Curve B is the combined White (1965) and Ellis (1970) curve used by Truesdell (1976a). Curves C and D show the approximate locations of the low albite-microcline and high albite-sanidine lines from figure 3 (from Fournier, 1979a).

Figure 8.--For the indicated starting compositions, the effect of dilution of hot water by cold water upon the calculated Na-K-Ca temperature. Different starting compositions will give different results.

Figure 9.--Graph for estimating magnesium temperature correction, ΩT_{Mg}, to be subtracted from the Na-K-Ca calculated temperature. $R = 100\ Mg/(Mg + Ca + K)$, expressed in equivalents. (From Fournier and Potter, 1979).

Figure 10.—Dissolved silica-enthalpy graph showing procedure for calculating the initial enthalpy of a high-temperature water that has mixed with a low temperature water (modified from Truesdell and Fournier, 1977).

Figure 11.—Enthalpy-composition diagram showing changes in concentration resulting from adiabatic cooling (boiling) with single stage steam separation. Points S_{100} and S_{200} show the enthalpies of steam at 100° and 200°C respectively. X is dissolved material (arbitrary units). See text for additional discussion.

Figure 12.—Enthalpy-chloride relations for waters from Upper Basin Yellowstone National Park. Small circles indicate Geyser Hill-type waters and small dots indicate Black Sand-type waters.

Figure 13.—Schematic model of conditions in a vapor-dominated geothermal system.

Figure 14.—Schematic model of conditions in a hot-water-dominated geothermal system where boiling temperatures prevail through a steeply dipping structure filled with water.

Figure 15.—Enthalpy-chloride relations for hot spring and well waters from selected localities listed in Table 2. 15a, Orakeikorako; 15b, Cerro Prieto; 15c, El Tatio; and 15d, Ahuachapán. (Numbers in diagrams correspond to columns in table 2.)

Figure 16.—Comparison of measured reservoir temperatures in wells and calculated reservoir temperatures using (a) silica, (b) Na/K, and (c) Na-K-Ca geothermometers applied to hot spring waters listed in Table 2. Triangles indicate waters that have cooled adiabatically, squares indicate conductive cooling, X indicates partly conductive and partly adiabatic cooling, and circles are mixtures of hot and cold water.

Figure 17.—Enthalpy-chloride relations for waters from a 114 m well at Coso Hot Springs, California.

Table 1.--Equations expressing the temperature dependence of some geothermometers based on dissolved constituents. Concentration C in mg/kg

GEOTHERMOMETER	EQUATION	RESTRICTIONS
a. Quartz-no steam loss	$t^{\circ}C = \frac{1309}{5.19 - \log C} - 273.15$	$t = 0^{\circ}C\text{-}250^{\circ}C$
b. Quartz-maximum steam loss	$t^{\circ}C = \frac{1522}{5.75 - \log C} - 273.15$	$t = 0^{\circ}C\text{-}250^{\circ}C$
c. Chalcedony	$t^{\circ}C = \frac{1032}{4.69 - \log C} - 273.15$	$t = 0^{\circ}C\text{-}250^{\circ}C$
d. α-Cristobalite	$t^{\circ}C = \frac{1000}{4.78 - \log C} - 273.15$	$t = 0^{\circ}C\text{-}250^{\circ}C$
e. β-Cristabalite	$t^{\circ}C = \frac{781}{4.51 - \log C} - 273.15$	$t = 0^{\circ}C\text{-}250^{\circ}C$
f. Amorphous silica	$t^{\circ}C = \frac{731}{4.52 - \log C} - 273.15$	$t = 0^{\circ}C\text{-}250^{\circ}C$
g. Na/K (Fournier)	$t^{\circ}C = \frac{1217}{\log (Na/K) + 1.483} - 273.15$	$t > 150^{\circ}C$
h. Na/K (Truesdell)	$t^{\circ}C = \frac{855.6}{\log (Na/K) + 0.8573} - 273.15$	$t > 150^{\circ}C$
i. Na-K-Ca	$t^{\circ}C = \frac{1647}{\log (Na/K) + \beta[\log(\sqrt{Ca}/Na) + 2.06] + 2.47} - 273.15$	$t < 100^{\circ}C$, $\beta = 4/3$ $t > 100^{\circ}C$, $\beta = 1/3$
j. $\Delta^{18}O(SO_4^{=}\text{-}H_2O)$	$1000 \ln \alpha = 2.88(10^6 T^{-2}) - 4.1$ $\alpha = \frac{1000 + \delta^{18}O(HSO_4^-)}{1000 + \delta^{18}O(H_2O)}$ and $T = {}^{\circ}K$	

	El Tatio, Chile				Ahuachapán, El Salvador				Reykjanes, Iceland		
Column No.	1	2	3	4	5	6	7	8	9	10	11
Feature	Well 11 Flashed	Well 11 At Depth[1]	Spg. 181	Spg. 244	Well Ah-1 Flashed	Well Ah-1 At Depth	Spg. F	Spg. M	Well 8 Flashed[2]	Well 8 At Depth[3]	Spg. Unnamed
Depth, m		894				1400				1754	
Temp °C	85	240	89.5	85	98	232	87	70	100	277	99
pH	6.98		6.9	7.30	7.4		8.0	6.8		6.1	6.2
SiO_2	748	526	122	269	663	490	114	235	988	636	544
Ca	208	146	170	274	416	308	201	29	3480	1530	2260
Mg	0.15	0.11	6	0.4	tr	tr	1	8	25	16	123
Na	4900	3450	2250	4330	6120	4530	768	378	14930	9610	14325
K	825	580	230	525	995	736	18	39	2095	1348	1670
Li	44.9	31.6	--	46	--	--	--	--	--	--	--
HCO_3[5]	41	29	36	27	29	21	52	377	4150[6]	2670[6]	5[6]
SO_4	32	23	36	27	28	21	224	35	47.9	30.8	206
Cl	8716	6130	4009	8126	11046	8172	1528	479	29930	19260	29100
F	--	--	--	--	--	--	--	--	.15	0.1	0.2
B	202	142	91	183	162	120	20	9.2	--	--	12
T SiO_2	256	257	148	201	247	250	145	191	279	275	232
T Na/K_{RF}	263	262	219	233	259	259	123	220	246	246	229
T Na/K_T	251	251	190	209	246	246	71	191	227	227	205
T Na-K-Ca	260	256	211	231	255	251	90	87	245	240	232
T Na-K-Ca-Mg	260	256	199		255	251	90	87		235	192
Cl/HCO_3		364	61	341		670	51	2.2		12.4	10013
Cl/SO_4		722	302	815		1054	18.5	2.2		1693	383
Cl/B		13.2	13.4	13.5		21	23	16		--	738
K/Li		3.27	--	2.03		--	--	--		--	--
Cl_{spg}/Cl_{depth}			0.65	1.33			0.19	0.06			1.51
Reference	9		9	9	10		10	10		11	11

T| .--C| son | spr| id wa| ers.| inued

	Cerro Prieto, Mexico					Broadlands, New Zealand			Ngawha, New Zealand		
Column No.	12	13	14	15	16	17	18	19	20	21	22
Feature	Well M-26 Flashed[4/]	Well M-26 At Depth[1/]	Spg. 41	Spg. 49	Spg. 54 Flashed	Well 2 Flashed	Well 2 At Depth[1/]	Onaki Pool	Well 1 Flashed	Well 1 At Depth[1/]	Jubilee Bath
Depth, m		1240					1030			585	
Temp °C	100	292	40	57	98	99	260	95	99	230	50
pH	8.0		2.40	6.50	7.4	8.3		7.05	7.4		6.5
SiO_2	1156	705	247	45	92	805	549	338	460	343	186
Ca	971	592	407	283	492	2.2	1.5	--	--	--	8
Mg	1	0.6	87	20	38	0.08	.07	--	--	--	2.5
Na	10467	6382	4100	1350	3700	1050	716	860	950	708	870
K	2544	1551	1010	233	400	224	143	82	80	60	79
Li	23.8	14.5	12.1	4.4	8	11.7	8.0	7.4	12.2	9.1	11
HCO_3	46	28	0	128	42	128[2/]	87	490[2/]	616[2/]	45	240[2/]
SO_4	<6	<3.5	690	960	130	8	5	100	17	13	500
Cl	19548	11918	8410	2930	6700	1743	1188	1060	1625	1211	1336
F	--	--	--	--	--	7.3	5.0	5.2	0.8	.6	0.3
B	22	13.4	--	--	--	48.4	32.9	32	1200	894	1020
T SiO_2	203	286	195	97	132	262	261	219	220	220	175
T Na/K_{gf}	300	300	302	265	223	280	280	213	203	204	209
T Na/K_T	308	308	310	254	196	277	276	182	170	170	177
T Na-K-Ca	289	282	277	228	213	294	238	--	--	--	216
T Na-K-Ca-Mg			161	178	164						169
Cl/HCO_3		732	--	39	274		23	3.7		46	9.6
Cl/SO_4		--	35	8.3	140		643	29		252	7.2
Cl/B		271	--	--	--		11	10		0.4	0.4
K/Li		19	15	9.4	8.9		3.2	2.0		1.2	1.3
Cl_{spg}/Cl_{depth}			0.71	0.25	0.56			0.89			1.10
Reference	12		13	13	13	14		15	15		15

Table 2.--Comparison of hot spring and well waters, Continued.

	Orakeikorako, New Zealand				Rotokawa, New Zealand			Chingshui, Taiwan		
Column No.	23	24	25	26	27	28	29	30	31	32
Feature	Well 2 Flashed	Well 2 At Depth[1]	Spg. 22	Spg. 66A	Well 2 Flashed	Well 2 At Depth[1]	Spg. 6	Well TC-4 Flashed	Well TC-4 At Depth[1]	Spg. 20
Depth, m		1150				880			1505	
Temp °C	99	260	99	64	99	220	654	100	195	99
pH	9.1		9.2	8.2	7.8		2.5	8.5		9.7
SiO_2	480	327	280	150	430	329	340	342	280	289
Ca	<1	<1	0.8	4.6	50	38	11	tr	tr	tr
Mg	--	--	--	0.6	--	--	11/3	tr	tr	tr
Na	550	375	370	135	1525	1168	990	1095	896	923
K	54	37	34	10	176	135	102	36	29	39
Li	3.1	2.1	3.4	1.2	10.2	7.8	7.8	7	6	--
HCO_3	2902/	198	113	201	556/	42	1446/	2807	2296	2586
SO_4	142	97	185	12	120	92	520	32.1	26.2	10.3
Cl	546	372	404	78	2675	2049	1433	18.3	15.0	6
F	5.7	3.9	10.8	2.9	676	5.1	--	--	--	
B	7.7	5.2	3.4	5.4	102	78	45	36	29	30
T SiO_2	223	216	187	161	215	217	219	200	204	198
T Na/K_{HF}	215	216	210	194	228	229	219	141	140	156
T Na/K_T	186	186	179	157	203	204	191	92	91	110
T Na-K-Ca	—	--	223	174	224	221	223	--	--	--
T Na-K-Ca-Mg				138			88			
Cl/HCO_3		3.2	6.2	0.69		84	17		.01	<.01
Cl/SO_4		10.4	5.9	17.6		60.4	7.5		1.55	1.58
Cl/B		22	36.2	4.4		8.0	9.7		0.16	.06
K/Li		3.1	1.8	1.5		3.1	2.3		0.9	--
Cl_{spg}/Cl_{depth}			1.09	0.21			0.70			0.38
Reference		17	17	17	15		15	18		19

Table 2.--Comparison of hot spring and well waters, Continued.

	Tuchang, Taiwan				Kizildere, Turkey		
Column No.	33	34	35	36	37	38	39
Feature	Well IT-3 Flashed	Well IT-3 At Depth[1/]	Spg. Unnamed	Spg. Unnamed	Well KD15 Flashed	Well KD15 At Depth[1/]	Spg. Unnamed
Depth, m		445				506	
Temp °C	100	173	60	96	99	205	100
pH	8.7		6.7	8.7	7.8		9.0
SiO_2	253	213	25	69	268	214	185
Ca	tr	tr	73	--	6	5	1.2
Mg	tr	tr	17	--	1.2	1.0	0.1
Na	1100	947	338	710	1172	935	1260
K	15.8	13.6	71	14.7	117	93	125
Li	--	--	--	--	--	--	--
HCO_3	2884	2484	1258	2010	2502	2000	2560
SO_4	36	31	82.3	32	778	621	750
Cl	21	18	14.2	13.4	112	89	103
F	--		--	--	16.9	13/5	18
B	30.5	26.3	--	--	25.6	20.4	23
T SiO_2	183	184	72	118	185	185	174
T Na/K_{RF}	99	99	117	116	217	216	216
T Na/K_T	44	44	64	64	187	187	187
T Na-K-Ca	--	--	73	--	231	228	251[1/]
T Na-K-Ca-Mg			73			217	
Cl/HCO_3		.01	.02	.01	.08	.08	.07
Cl/SO_4		1.57	0.47	1.13		0.39	1.36
Cl/B		0.21	--	--		1.33	1.36
K/Li		--	--	--		--	--
Cl_{spg}/Cl_{depth}			0.79	0.74		--	--
Reference	18		19	19	20		

Table 2.--Comparison of hot spring and well waters, Continued.

Column No.	40	41	42	43	44	45
	Yellowstone Park, United States					
Feature	Well Y3 Flashed[2]	Well Y3 At Depth[3]	Ojo Caliente	Well Y8 Flashed[2]	Well Y8 At Depth[3]	Rusty Geyser
Depth, m		88			64	
Temp °C	92	174	95	92	169[8]	92
pH		8.12	8.31		7.9	8.8
SiO_2		--	230	302	258	297
Ca	1.49	1.26	1.1	1.4	1.2	.29
Mg	.02	.02	.02	.05	.04	<.01
Na	319	270	317	421	360	408
K	13	11	9.2	17.5	15	19
Li	4.1	3.5	4.5	3.0	2.6	2.7
HCO_3	209	177	249	516	493	573
SO_4	22/6	19/1	27	19	16	17
Cl	329	278	331	281	280	292
F	35	30	33	30	26	29
B	4.3	3.6	4.0	3.0	2.6	3.0
T SiO_2			176	192	198	191
T Na/K_{RF}	154	154	134	155	155	162
T Na/K_T	108	108	84	109	109	118
T Na-K-Ca	167	166	153	174	172	194
T Na-K-Ca-Mg						
Cl/HCO_3		2.7	2.3		0.84	0.88
Cl/SO_4		39	33		41	47
Cl/B		24	25		28	30
K/Li		0.6	0.4		1.0	1.3
Cl_{spg}/Cl_{depth}			1.19			1.22
Reference	22		22	23		23

Footnotes for table 2

1/ Composition calculated from analysis of flashed sample.

2/ Composition calculated from analysis of downhole sample.

3/ Collected using a down-hole sampler, Ave. 11 samples.

4/ Sample collected after flashing at 670 kPa. Analysis recalculated to flashing at 100 kPa.

5/ Total HCO_3^- and $CO_3^=$ recalculated to HCO_3^-.

6/ Total CO_2 recalculated to HCO_3^-.

7/ Estimated temperature probably is much too high owing to the precipitation of $CaCO_3$.

8/ The well apparently intersected a fracture that tops a deeper reservoir with a temperature of about 190° to 200°C.

9/ Cusicanqui and others (1976)

10/ Romagnoli and others (1976)

11/ Bjornsson and others (1972)

12/ Reed (1976)

13/ Mercado (1968)

14/ Mahon and Finlayson (1972)

15/ Ellis and Mahon (1977)

16/ Ellis (1966)

17/ Mahon in Lloyd (1972)

18/ Mining Research & Seveice Organization (1977)

19/ Personal communication, MRSO (1977)

20/ MTA Pamphlet

21/ Dominco and Samilgil (1970)

22/ Bargar and others (1973)

23/ Unpublished data, U. S. Geological Survey

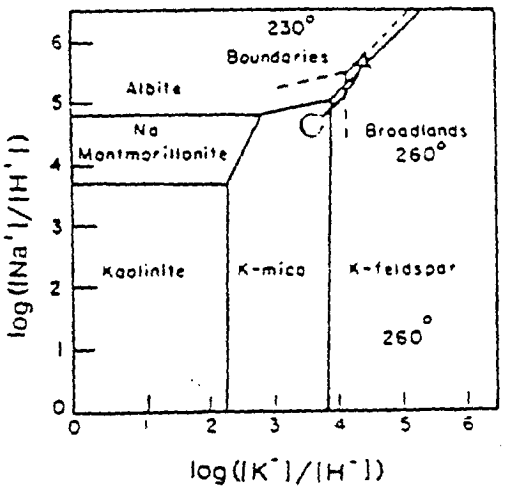
230°
Boundaries
Albite
Na
Montmorillonite
Broadlands
260°
Kaolinite
K-mica
K-feldspar
260°
log([Na⁺]/[H⁺])
log([K⁺]/[H⁺])
0
1
2
3
4
5
6

FIGURA 1.

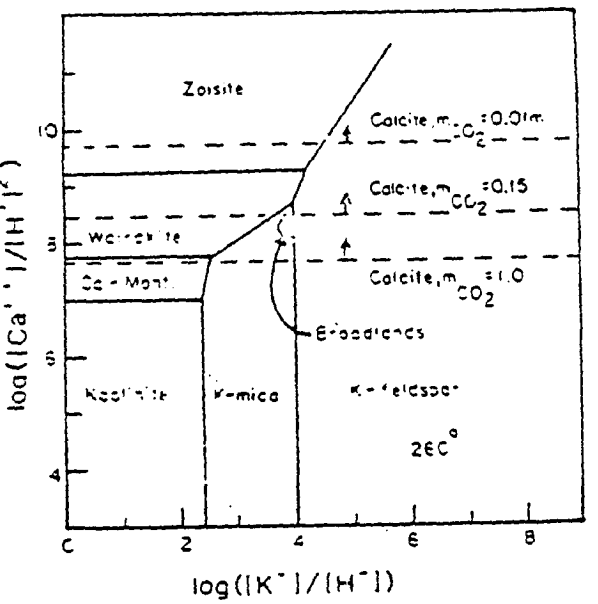
Zoisite
Calcite, m_{CO_2} = 0.01m
Calcite, m_{CO_2} = 0.15
Calcite, m_{CO_2} = 1.0
Wairakite
Ca - Mont.
Kaolinite
K-mica
K-feldspar
25C°
10
8
6
4
0
2
4
6
8
log([K⁺]/[H⁺])
log([Ca⁺⁺]/[H⁺]²)

FIGURA 2.

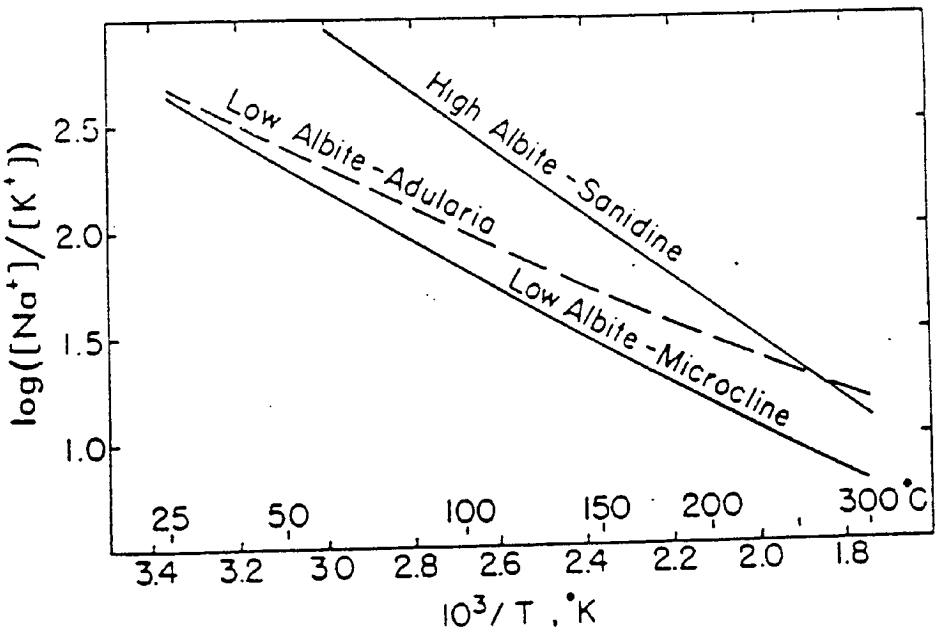
High Albite - Sanidine
Low Albite - Adularia
Low Albite - Microcline
log([Na+]/[K+])
2.5
2.0
1.5
1.0
25
50
100
150
200
300°C
3.4
3.2
3.0
2.8
2.6
2.4
2.2
2.0
1.8
10³/ T , °K

FIGURA 3.

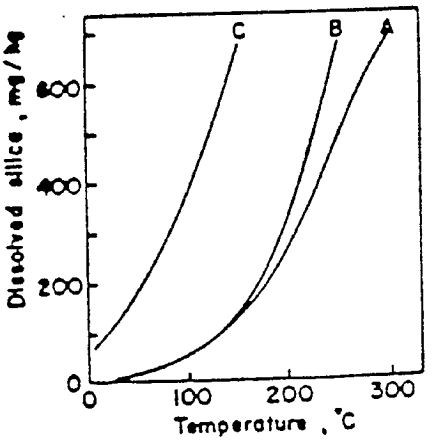
C
B
A
600
400
200
0
0
100
200
300
Dissolved silica , mg/kg
Temperature , °C

FIGURA 4.

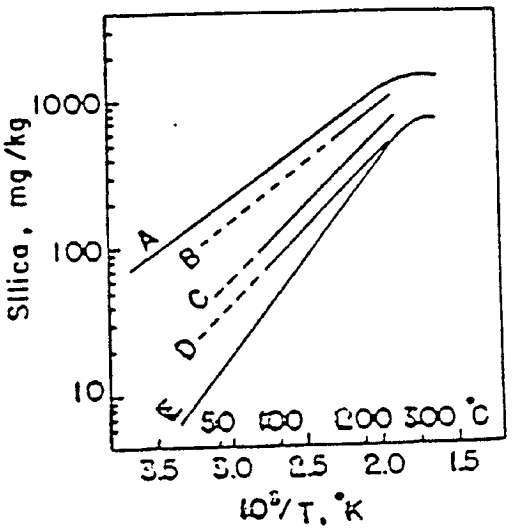

FIGURA 5.

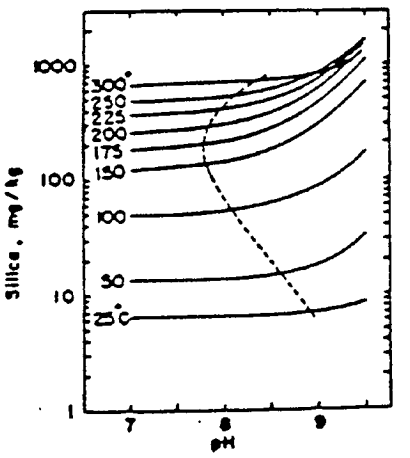

FIGURA 6.

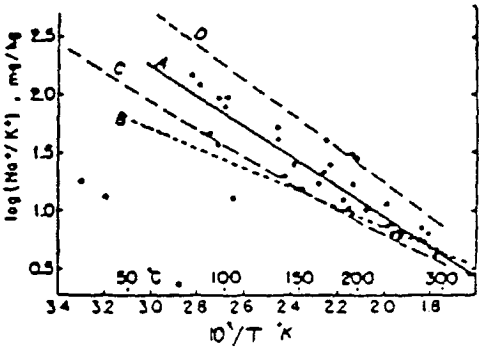

FIGURA 7.

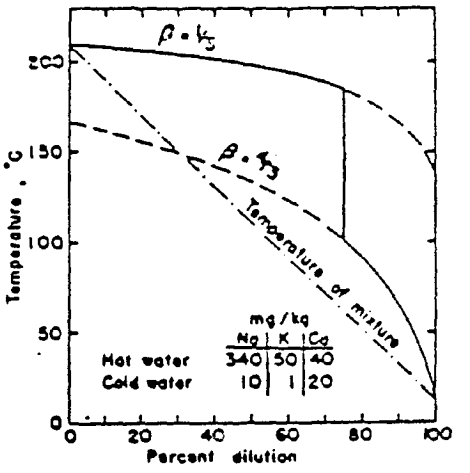

FIGURA 8.

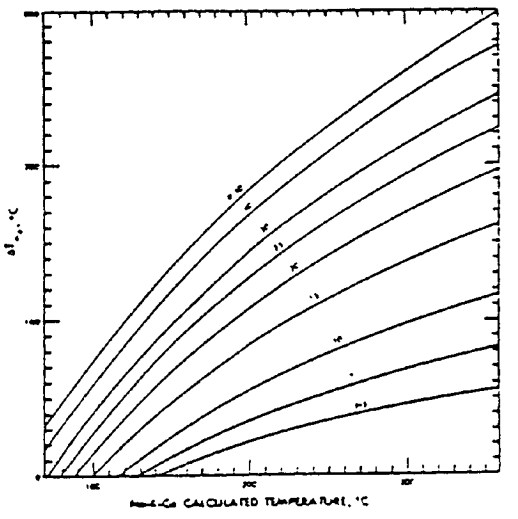

FIGURA 9.

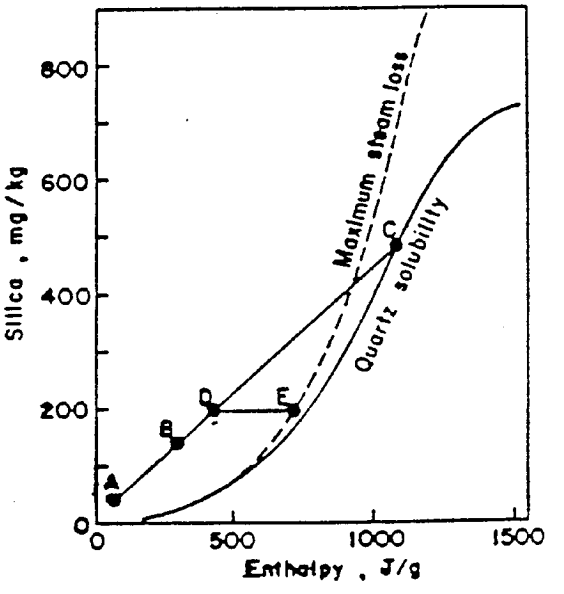

FIGURA 10.

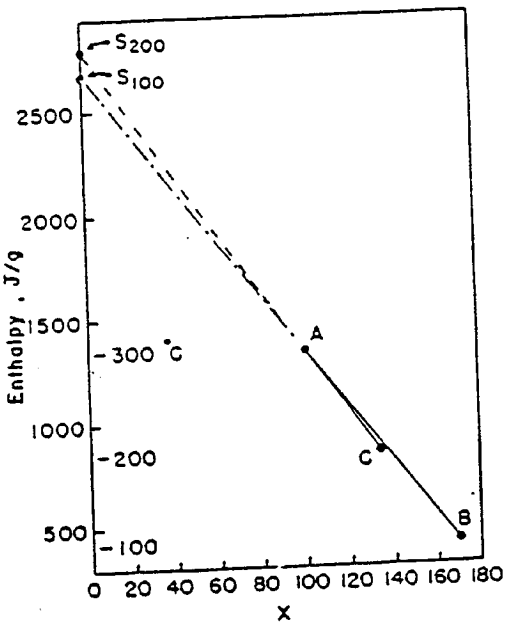
S200
S100
2500
2000
Enthalpy , J/g
1500
300 °C
1000
200
500
100
A
C
B
0 20 40 60 80 100 120 140 160 180
X

FIGURA 11.

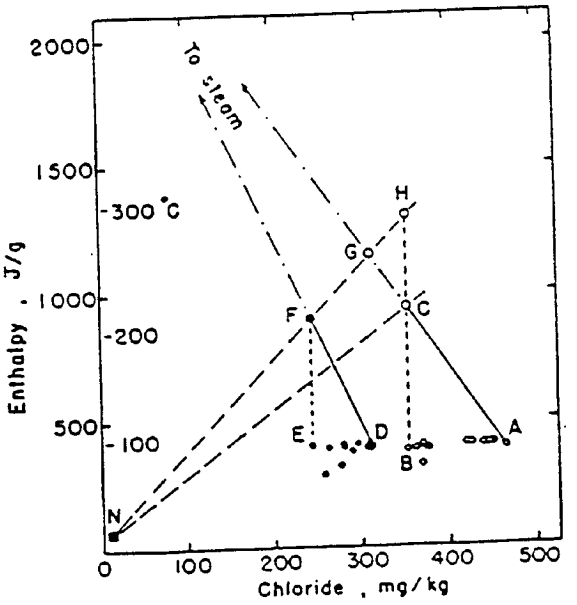
2000
1500
1000
500
Enthalpy , J/g
To steam
300 °C
200
100
H
G
F
C
E
D
B
A
N
0
100
200
300
400
500
Chloride , mg/kg

FIGURA 12.

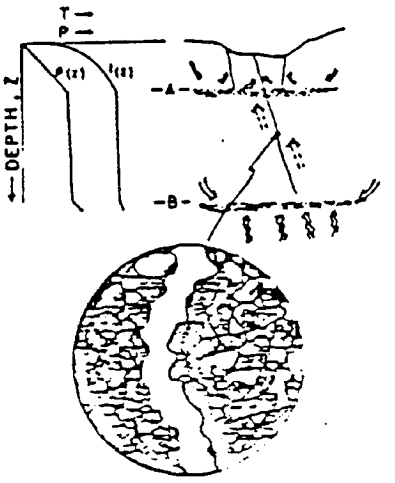

FIGURA 13.

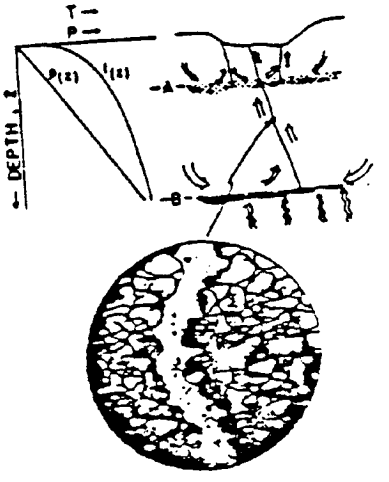

FIGURA 14.

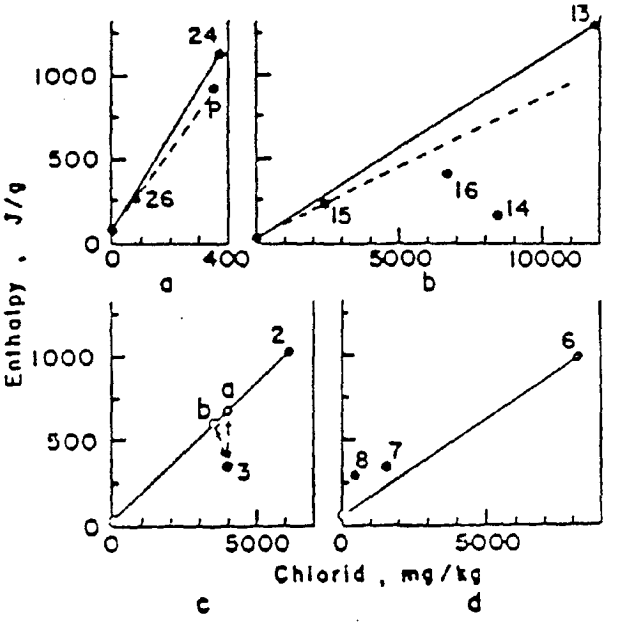

FIGURA 15.

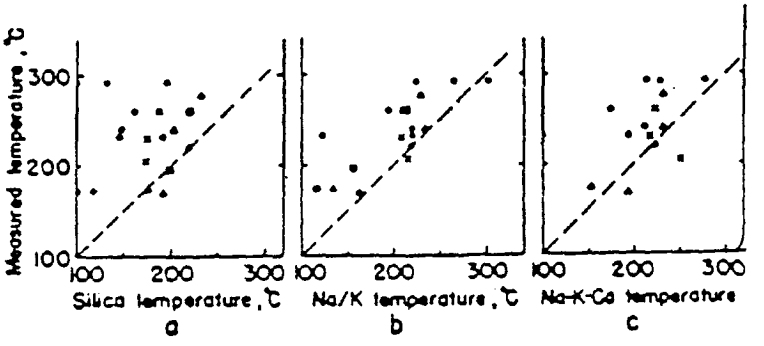

FIGURA 16.

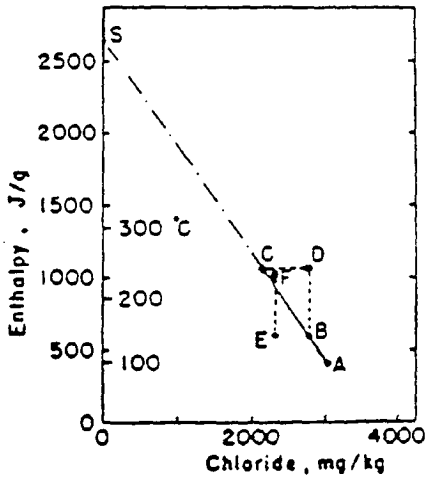
S
2500
2000
1500
1000
500
0
300 °C
200
100
C
D
F
E
B
A
0
2000
4000
Enthalpy , J/g
Chloride , mg/kg

FIGURA 17.